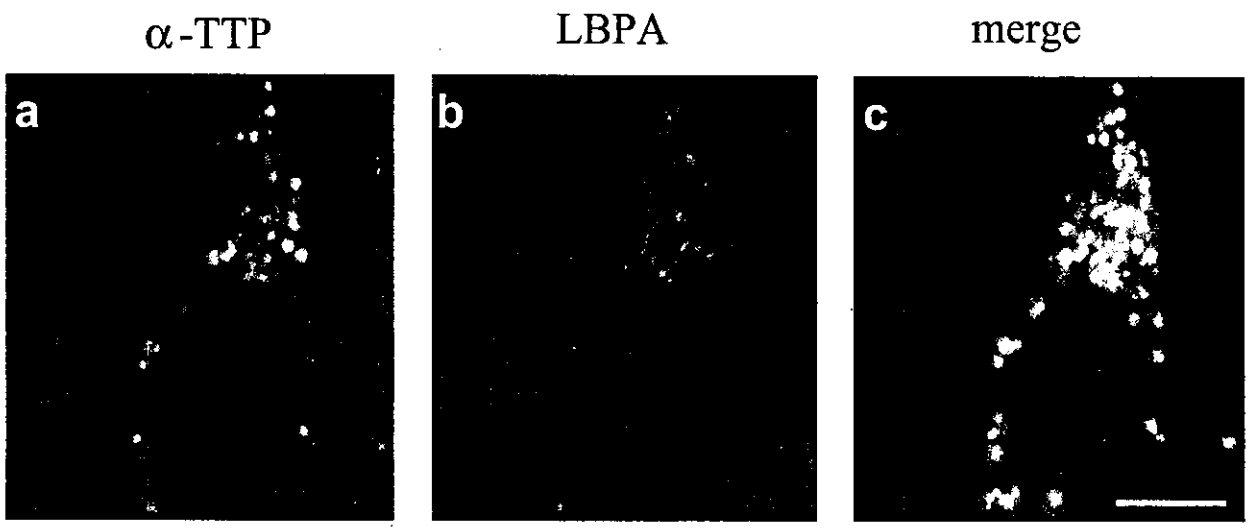

Figure 5 Co-localization of α-TTP and LBPA after chloroquine treatment. McA-TTP cells were incubated for 4 h with 100 μM chloroquine and immunostained with rabbit polyclonal antibody against α-TTP and mAb against LBPA. The secondary antibodies used are Alexa 488 goat anti-rabbit antibody (green) and Alexa 546 goat anti-mouse antibody (red). Bar, 10 μm.

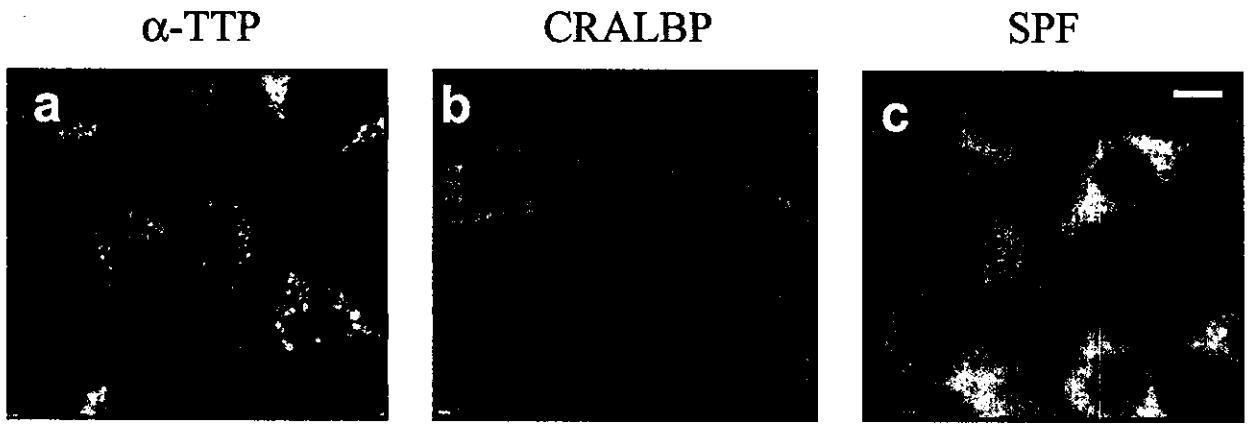

Figure 6 α-TTP versus SPF and CRALBP localization after chloroquine treatment. McARH7777 cells transiently expressing myc-tagged α-TTP (a), CRALBP (b) and SPF (c) were prepared as described in Experimental procedures. The cells were incubated for 4 h with 100 μM chloroquine and immunostained with anti-myc mAb. Note that addition of myc epitope at the N-terminus of α-TTP does not affect the chloroquine-induced compartmentalization. Bar, 10 μm.

localization of α-TTP in hepatic parenchymal cells is also observed in cells from other origins. Chinese hamster ovary (CHO) cells were transiently transfected with myc-tagged α-TTP and incubated for 24 h, followed by 4 h chloroquine treatment. α-TTP remained in the cytosol of CHO cells, identical results were also found in HeLa and COS-7 cells (unpublished data). These data suggested that pH-dependent translocation of α-TTP only occurred in hepatic parenchymal cells, making it likely that a specific α-TTP target solely localized in hepatocyte late endosomes exists.

The N-terminal portion of α-TTP is obligatory for pH-dependent localization

α-TTP contains 278 amino acids. A region between amino acid residues 78 and 214 is considered to be the lipid-binding region (SMART program package, http://smart.embl-heidelberg.de/). So far, no specific functions of other α-TTP regions are known. To gain information on which α-TTP domain is required for accumulation in late endosomes, we examined the N- and C-terminal regions of α-TTP excluding the lipid-binding domain.

Almost none of the deletion constructs of the α-TTP N- and C-termini showed stable expression. We therefore focused on creating a chimeric protein instead. As shown above, CRALBP remains in the cytosol even after chloroquine treatment. To elucidate differences in chimeric proteins with and without chloroquine-induced accumulation, we created several chimeric proteins of α-TTP and CRALBP. Figure 7A gives a schematic summary of the plasmids encoding wild-type α-TTP and CRALBP, as well as the diverse chimeric forms used for this study. We studied eight chimeric proteins of which CT1 and CT6 were expressed stably. To determine the ability of α-tocopherol-binding to CT1 and CT6 compared with α-TTP and CRALBP, α-[^{14}C]tocopherol-enriched liposomes were mixed with the respective proteins, followed by gel filtration. Radio-labelled α-tocopherol was eluted simultaneously with α-TTP, CT1 and CT6 (data for α-TTP and CT6 shown in Fig. 7B), while this phenomenon was not seen with CRALBP (unpublished data).

Next, the late endosomal localization after chloroquine treatment for the created chimeric proteins CT1 and CT6 was determined. Myc-tagged chimeric proteins were transfected transiently into McARH7777 cells and immunofluorescence studies with anti-myc antibody were performed. Accumulation of CT1, but not CT6, after chloroquine treatment was seen, similar to α-TTP (Fig. 7C). Therefore, a region within 21–50 was regarded to be necessary for chloroquine-induced α-TTP localization.

Discussion

The current experiments show that α-TTP, a cytosolic lipid-binding/transfer protein, accumulates in late endosomes in a hepatocyte-derived cell line and in hepatocytes per se after chloroquine treatment. The inhibition of α-tocopherol secretion from hepatocytes by chloroquine is likely due to the binding of cytosolic α-TTP to late endosomal membranes, thereby impairing the transfer capacity of α-TTP for α-tocopherol. Several observations point to the possibility that α-TTP is mainly localized in the cytosolic surface of late endosomal membranes. In wash-out experiments, it is evident that α-TTP re-localizes in the cytosol after showing punctated accumulation in the chloroquine treatment phase. Furthermore, the α-TTP expression level shows no significant change prior to, during and after chloroquine treatment. This suggests that α-TTP is not degraded in late endosomes, but is capable of being transferred from cytosol to the late endosomal surfaces and vice versa. As α-TTP is recovered from the soluble fraction upon fractionation of the cells after chloroquine treatment and not from the membrane fraction (unpublished data), only a weak affinity of α-TTP to late endosomal membranes can be postulated. It can be stated that this phenomenon only takes place in the hepatocyte or hepatocyte-derived cells, and, of the cytosolic lipid-binding/transfer protein family to which α-TTP belongs, only α-TTP is shown to have this binding capacity. Therefore, we hypothesize that α-TTP has a specific, hepatic target molecule localized in late endosomal membranes which is necessary for its binding under the given conditions.

It is unlikely that α-TTP undergoes some modification in the cytosol by the action of chloroquine or bafilomycin A1 that makes it translocate to late endosomal membranes. More plausible is the possibility that the intraendosomal pH rise or change in proton gradient between cytosol and endosomal lumen caused by chloroquine treatment leads to a conformational change of the putative endosomal target protein, which then expresses its binding domain for α-TTP at the cytosolic surface of late endosomes. In this context, the following reported experiments are noteworthy: when lactoperoxidase-conjugated asialoorosomucoid is endocytosed by Hep-G2 cells and endosomal membrane proteins are specifically labelled with ^{125}I, the labelled protein pattern is altered when the intraendosomal pH is changed (Watts 1984). This implies that conformational changes of late endosomal membrane proteins take place when pH changes occur.

Further reports of cytosolic proteins interacting with endosomal membranes under conditions changing the endosomal pH are known (Aniento *et al.* 1996). Formation of transport vesicles at early endosomal membranes is regulated by coat protein (COP). Recruitment of COP on the membrane is a process dependent on the acidic milieu of early endosomes. βCOP, a component of the COP coat, is present on early endosomes and is required for the formation of the vesicular intermediates destined for late endosomes. Association of βCOP with the membrane is dependent on the lumenal pH, and neutralization of the endosomal pH blocks βCOP association to endosomal membranes. These data also suggest the presence of a specific target which is pH sensitive, and thus serves as a sensor of the endosomal pH.

By no means, however, is there any evidence that the target molecule in late endosomal membranes is a protein. Recently, it has been reported that α-TTP not only binds α-tocopherol, but also polyphosphinositides (Krugmann *et al.* 2002). Hawkins and colleagues demonstrated that α-TTP binds to phosphatidylinositol-3,4- and 3,5-diphosphate-derivatized beads. Interestingly, other members of the Sec14 family, such as MEG-2

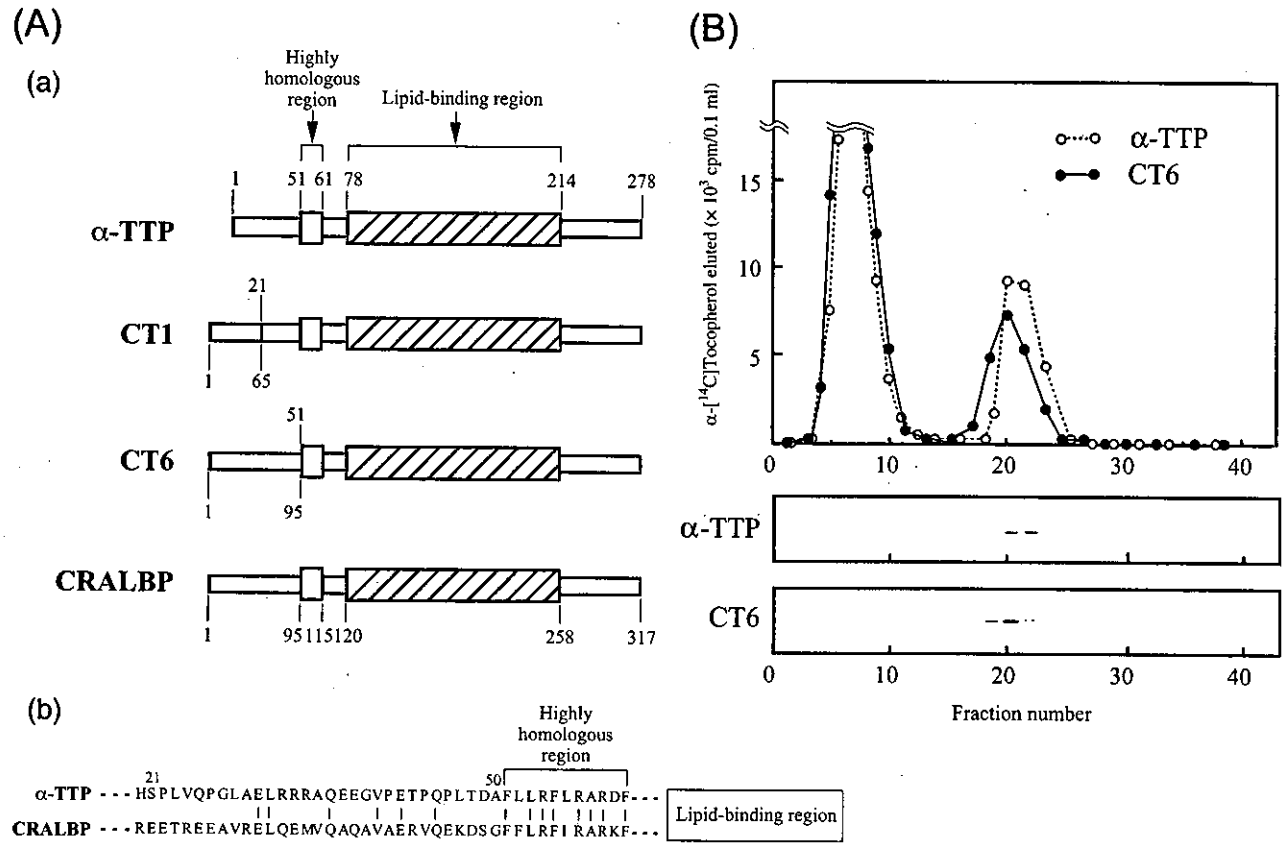

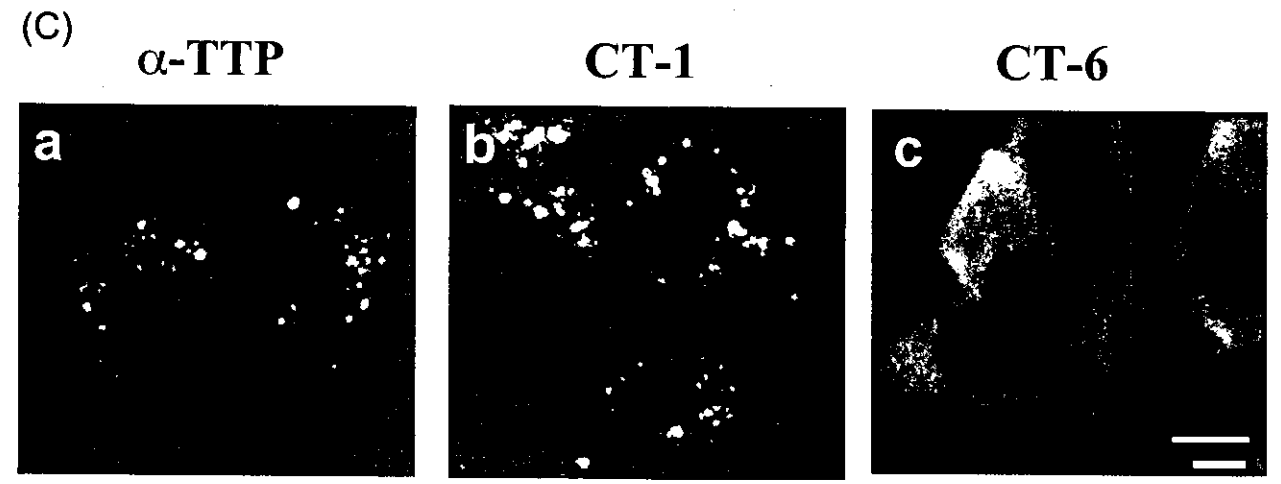

Figure 7 Identification of domains in α-TTP relevant for late endosomal translocation. (A) Structure of α-TTP, chimeric forms CT1 and CT6, and CRALBP. Upper numbers indicate amino acid sequence of α-TTP, lower numbers of CRALBP. In the CT1 chimeric form, a sequence of 20 amino acids from the N-terminal of α-TTP was exchanged by the corresponding N-terminal sequence of CRALBP and in the CT6 chimeric form, the first 50 amino acids from the N-terminal were exchanged. A myc-tag was attached at the N-termini of all constructs. (B) Assays for α-tocopherol binding were carried out as described in Experimental procedures. Briefly, the supernatant obtained from McARH7777 cells expressing α-TTP or CT6 were incubated with α-[^{14}C]tocopherol-containing liposomes and then subjected to gel filtration column chromatography. Each fraction was subjected to radiolabel assay and Western blotting. After the void fractions containing most of α-[^{14}C]tocopherol-containing liposomes, one peak was observed in the α-TTP and CT6 assays, respectively. (C) Cell localization of α-TTP (a), CT1 (b) and CT6 (c) after chloroquine treatment. Cells were incubated with 100 μM chloroquine and immunostained with anti-myc mAb. Bar, 10 μm.

and Cdc42GAP also bind to polyphosphoinositide-derivatized beads. Ssh1p and Ssh2P, members of the soy bean Sec14 family, bind polyphosphoinositides (Kearns *et al.* 1998b). In fact, Sec14 itself recognizes phosphatidylinositol and phosphatidylcholine and regulates phosphatidylcholine metabolism. Although the physiological function of α-TTP binding to polyphosphoinositides is so far unknown, it is possible that intracellular organelle targeting is the explanation for this binding capacity.

Members of the Sec14 family all have molecular weights of 30 kDa or more and an amino acid sequence of approximately 150 amino acids is responsible for the lipid-binding domain in Sec14 family members. Other regions are likely to have diverse cellular functions besides lipid-binding, but in most Sec14 family members, no specific function of domains besides the Sec14 domain have been described. CRALBP, for example, has a far longer N-terminal region than α-TTP and SPF has a C-terminal region, called jelly roll domain, which is also far longer than the corresponding region in α-TTP. In this study, we have identified the amino acid region relevant for late endosomal targeting, located in the α-TTP amino acid sequence 21–50. This region is next to the N-terminal side of a domain highly conserved throughout the Sec14 family, to which no function could be attributed so far (Fig. 7A.b). It is noteworthy that CRALBP, which does not contain an amino acid sequence similar to 21–50 of α-TTP, shows no translocation capacity as described here for α-TTP. The 21–50 amino acid sequence is relatively rich in charged amino acids such as arginine and glutamic acid as well as proline and will most likely give hints for the elucidation of this late endosomal target molecule in future.

We previously demonstrated in experiments using [^{14}C]tocopheryl acetate that a hepatoma cell line expressing α-TTP secreted α-tocopherol more efficiently than cells lacking α-TTP, and that α-TTP-stimulated α-tocopherol secretion is not coupled to the VLDL secretion pathway. More recently, Oram *et al.* (2001) showed that an ATP-binding cassette transporter called ABCA1 which transports cholesterol and phospholipids out of the cell also mediates secretion of cellular α-tocopherol from hepatocytes. The best explanation of the mechanisms by which hepatic α-tocopherol transport is mediated by α-TTP is as follows: α-tocopherol endocytosed with circulating plasma lipoproteins is transported to late endosomes/lysosomes, where the lipoproteins are hydrolysed, thereby releasing α-tocopherol. α-Tocopherol is then trapped by cytosolic α-TTP, transported to the plasma membrane directly or indirectly and finally secreted into the circulation by an ABC-transporter present in hepatocyte plasma membranes. This hypothesis, however, lacks the explanation of how α-tocopherol released into the lumen of acidic compartments can be bound by the cytosolic α-TTP. While our experiments are conducted under non-physiological conditions, i.e. elevation of late endosomal pH, they nevertheless hint at the existence of a specific target for α-TTP on late endosomal membranes. It can be speculated that, under physiological conditions, the affinity between the putative target molecule and α-TTP is very low and that their interaction is of a transient nature. This mechanism may be responsible for the transfer of α-tocopherol between late endosomes and cytsolic α-TTP.

The only well-studied mechanism involving lysosomal lipid transport is the transport of cholesterol. Exogenous cholesterol internalized into cells through the endocytotic uptake of lipoproteins is transported to late endosomes/lysosomes where the hydrolysis of cholesteryl esters releases free cholesterol for rapid distribution to the plasma membrane and other intracellular sites (Brown & Goldstein 1986; Liscum & Dahl 1992). The transfer of cholesterol derived from late endosomes/lysosomes to other organelles such as the endoplasmic reticulum and plasma membrane has been shown to be mediated by Niemann-Pick disease type C class 1 (NPC1), a multiple membrane spanning protein (with 16 transmembrane domains) consisting of 1278 amino acids Although the precise mechanism of cholesterol transport by NPC1 is yet unclear, it has recently been suggested that vesicles containing NPC1 and cholesterol bud from late endosomes and finally fuse with perinuclear and peripheral membranous compartments. A vesicular transport mechanism is therefore likely to function in transporting cholesterol from late endosomes/lysosomes. Traber *et al.* (1994) have estimated that 30–50% of hepatic α-TTP are in fact involved in hepatocyte α-tocopherol transport *in vivo*. Under physiological conditions, one LDL particle contains approximately 1500–2000 cholesterol molecules, 100× more than α-tocopherol molecules. After endocytosis of LDL in late endosomes/lysosomes, unesterified cholesterol and α-tocopherol are released. If a similar cytosolic carrier protein should exist for cholesterol, this protein must have a 100× (or at least 30–50×) higher concentration of α-TTP. As rat liver α-TTP amounts to 1/500th of total cytosolic protein (Sato *et al.* 1991), this cholesterol carrier protein would have to make out one-fifth of total cytosolic protein, if it is to show the same transport capacity as α-TTP. No such cytosolic protein existing in such abundant amounts has been identified in the hepatocyte. Therefore, a far more effective vesicular transport mechanism should be necessary for transporting cholesterol from late endosomes/lysosomes. This transport mechanism is most

likely the above-mentioned transport mediated by NPC1-containing vesicles.

In preliminary experiments, we exposed ICR mice to oral chloroquine (300 mg/kg body weight) and after 6 h, plasma α-tocopherol and cholesterol levels were determined. We observed that chloroquine treatment caused a significant reduction of vitamin E levels by about 50%. However, no reduction of plasma cholesterol levels was seen. The mechanism of chloroquine-induced α-TTP accumulation therefore is likely to take place *in vivo* as well. Under physiological conditions, it is unlikely that a pH rise in late endosomes may occur, but under certain pathological conditions, this phenomenon is possible. Such a pathological condition exists in haemochromatosis, a genetic disease characterized by the accumulation of iron within organs, including the liver. A major feature of this disease is the selective sequestration of excess iron in hepatocyte lysosomes (Seyer & Peters 1978). Experimental iron overload in rats causes an increase in intralysosomal pH (Myers *et al.* 1991). It is interesting to note that patients with haemochromatosis show significantly low serum vitamin E levels, but normal serum lipid levels. These patients show normal liver function and no, or only minimal signs of, liver cell damage (elevated bilirubin and transaminase levels) (von Herbay *et al.* 1994). It is reasonable to assume that the loss of vitamin E in these patients could be due to enhanced formation of reactive oxygen species, which in turn induce the consumption of vitamin E. We hypothesize that an increase in late endosomal pH induces the accumulation of hepatic α-TTP in late endosomes, leading to impaired α-TTP function and finally to decreased serum vitamin E levels.

Experimental procedures

Cell cultures, pharmacological reagents, immunological reagents, and animals

The rat hepatoma cell line McARH7777 (American Type Culture Collection) was grown in Dulbecco's modified Eagle's medium with 10% FCS and 10% foetal horse serum containing 100 U/mL penicillin, 100 μg/mL streptomycin sulphate and 2 mM L-glutamine. McA-TTP cells were cultured in the same fashion as McARH7777, previously described (Arita *et al.* 1997). Primary hepatocyte cultures were obtained as previously described (Kim *et al.* 1996a). Chinese hamster ovary (CHO) cells were cultured in Ham's F-12 medium with 10% FCS containing 100 U/mL penicillin, 100 μg/mL streptomycin sulphate and 2 mM L-glutamine. Cycloheximide and brefeldin A were purchased from Wako Pure Chemical (Osaka, Japan), nocodazole, wortmannin, chloroquine and FITC-BSA were purchased from Sigma (Tokyo, Japan). α-Tocopherol was a gift from Eisai (Tokyo, Japan). α-[^{14}C]Tocopheryl acetate was synthesized as previously described (Nakamura & Kijina 1972). The mouse anti-rat monoclonal antibody against α-TTP (AT-R1) (Sato *et al.* 1993) or anti-myc mAb was used for the immunofluorescence studies together with fluorescent Alexa 594 goat anti-mouse antibody from Molecular Probes (Eugene, OR, USA) as a secondary antibody. The monoclonal antibody against LBPA (Kobayashi *et al.* 1998) was kindly provided by Dr Kobayashi (RIKEN, Saitama, Japan).

Cell transfection

Transient over-expression of myc-tagged rat α-TTP, human CRALBP or rat SPF in McARH7777 cells was carried out as follows: the cells were plated on day 0 at densities of 5×10^4 cells/24 wells on collagen-coated coverslips or 1×10^6 cells/100-mm collagen-coated dishes. On day 1, cells were transfected by Superfect transfection reagent (Qiagen, Chatsworth, CA, USA). After 3 h, fresh medium was added. Immunofluorescence was carried out 24 h thereafter. Human cDNA for CRALBP was amplified by RT-PCR using a human brain cDNA library as template DNA based on the sequence information in the database (GenBank/EMBL/DDBS accession no. 000317). A myc-tag was added at the N-termini of α-TTP, CRALBP or SPF in the transient transfection experiments.

Indirect immunofluorescence

McARH7777 cells were seeded on to coverslips and transfected as described above (transient transfectants), while McA-TTP cells (stable transfectants) and primary rat hepatocytes were cultured on collagen-coated coverslips in 24 wells (5×10^4 cells/well) and directly fixed as described in the following. McARH7777 cells were fixed on day 2, and McA-TTP cells on day 1 after washing in phosphate-buffered saline (PBS). Fixation was carried out with PBS containing 3.6% (wt/vol) formaldehyde for 30 min at room temperature (25 °C). Following three washes in PBS, cells were permeabilized in 100% methanol for 2 min/at 20 °C. The methanol solution was removed, and three washes in PBS followed. After blocking with PBS containing 3% BSA (PBS/BSA) for 30 min at room temperature, mAb AT-R1 at a dilution of 1 : 1000 with PBS/BSA in the case of stable transfectants, and rat hepatocytes and murine anti-myc mAb at a dilution of 1 : 2000 in the case of transient transfectants were used for 2 h-incubation at room temperature. The coverslips were washed twice in PBS for 5 min each and then incubated with fresh PBS/BSA containing 10% goat serum (Sigma) and the above mentioned secondary antibody at a dilution of 1 : 2000 for 1 h at room temperature. The fluorescent antibody was removed, and coverslips were washed three times at room temperature with PBS for 5 min and mounted on microscope slides with PermaFluor Aqueous Mounting Medium (Immunon, Pittsburgh, PA, USA). Fluorescence microscopy was performed with a Olympus Fluoview confocal microscope. Photomicrographs were digitally visualized with Adobe Photoshop™ 5.0 J software for Macintosh.

α-tocopherol secretion and binding assay

For the α-tocopherol secretion assay, McA-TTP cells were seeded at a density of 5×10^4 cells into 24-well collagen coated plates. After removing the medium, cells were incubated at 37 °C for 4 h in 0.5 mL of medium with α-[^{14}C]tocopheryl acetate-containing liposomes (0.05 μCi per well), which were made according to previously described methods (Arita *et al.* 1997). α-Tocopherol secretion (%) was calculated as shown in the legend for Fig. 1.

The α-tocopherol binding assay was performed as follows: McARH7777 cells were seeded at a density of 2×10^6 cells per 100 mm collagen-coated dish and, after transient transfection of α-TTP cDNA or CT1 or CT6 chimera cDNAs and 48 h incubation at 37 °C, cells were harvested and suspended in 250 μL PBS. Cell disruption was performed using a Branson Sonifier Cell Disruptor 185 (Branson Ultrasonics, Saitama, Japan), after which centrifugation at 100 000 *g* for 1 h at 4 °C followed. Two hundred microlitres of the supernatant was mixed with 25 μL of multilamellar liposomes; the preparation is described elsewhere (Nishikawa *et al.* 1990). The composition of liposomes is as follows: phosphatidylcholine/dicethyl phosphate/buthylhydroxytoluene/α-[^{14}C]tocopherol (1.5 Ci/mmol) (molar ratio 75 : 7.5 : 4 : 0.6). After 30-min incubation at 37 °C, the fraction (200 μL) was applied to a Superose 12 HR 10/30 column (Amersham Pharmacia, Tokyo, Japan), fractions were collected, and of each fraction, Western blotting and radioactivity measurements were performed.

Expression vectors for wild-type and chimeric versions of α-TTP and CRALBP

Wild-type plasmids α-TTP and CRALBP were constructed by ligating the mammalian expression vector pcDNA3 (Invitrogen, Tokyo, Japan) with the respective cDNA at *Eco*RI-*Sal*I sites, after which they were myc-tagged at the *Eco*RV-*Eco*RI sites. For constructing the chimeric proteins, a pcDNA plasmid was cut at its *Eco*RI-*Sal*I site and an α-TTP DNA fragment missing either 60 or 150 base pairs from 5′ was inserted. This procedure was followed by insertion of diverse CRALBP fragments to create the chimeric proteins CT1 and CT6.

References

Aniento, F., Gu, F., Parton, R.G. & Gruenberg, J. (1996) An endosomal β COP is involved in the pH-dependent formation of transport vesicles destined for late endosomes. *J. Cell Biol.* **133**, 29–41.

Arita, M., Nomura, K., Arai, H. & Inoue, K. (1997) α-tocopherol transfer protein stimulates the secretion of α-tocopherol from a cultured liver cell line through a brefeldin A-insensitive pathway. *Proc. Natl. Acad. Sci. USA* **94**, 12437–12441.

Brown, M.S. & Goldstein, J.L. (1986) A receptor-mediated pathway for cholesterol homeostasis. *Science* **232**, 34–47.

Chen, H.W. & Leonard, D.A. (1984) Chloroquine inhibits cyclization of squalene oxide to lanosterol in mammalian cells. *J. Biol. Chem.* **259**, 8156–8162.

Crabb, J.W., Nie, Z., Chen, Y., *et al.* (1998) Cellular retinaldehyde–binding protein ligand interactions. Gln-210 and Lys-221 are in the retinoid binding pocket. *J. Biol. Chem.* **273**, 20712–20720.

Gotoda, T., Arita, M., Arai, H., *et al.* (1995) Adult-onset spinocerebellar dysfunction caused by a mutation in the gene for the α-tocopherol-transfer protein. *N. Engl. J. Med.* **333**, 1313–1318.

von Herbay, A., de Groot, H., Hegi, U., Stremmel, W., Strohmeyer, G. & Sies, H. (1994) Low vitamin E content in plasma of patients with alcoholic liver disease, hemochromatosis and Wilson's disease. *J. Hepatol.* **20**, 41–46.

Hosomi, A., Arita, M., Sato, Y., *et al.* (1997) Affinity for α-tocopherol transfer protein as a determinant of the biological activities of vitamin E analogs. *FEBS Lett.* **409**, 105–109.

Intres, R., Goldflam, S., Cook, J.R. & Crabb, J.W. (1994) Molecular cloning and structural analysis of the human gene encoding cellular retinaldehyde-binding protein. *J. Biol. Chem.* **269**, 25411–25418.

Kayden, H.J. & Traber, M.G. (1993) Absorption, lipoprotein transport, and regulation of plasma concentrations of vitamin E in humans. *J. Lipid Res.* **34**, 343–358.

Kearns, B.G., Alb, J.A.J.R. & Bankaitis, V.A. (1998b) Phosphatidylinositol transfer proteins: the long and winding road to physiological function. *Trends Cell Biol.* **8**, 276–282.

Kearns, M.A., Monks, D.E., Fang, M., *et al.* (1998a) Novel developmentally regulated phosphoinositide binding proteins from soybean whose expression bypasses the requirement for an essential phosphatidylinositol transfer protein in yeast. *EMBO J.* **17**, 4004–4017.

Kim, H.S., Arai, H., Arita, M., *et al.* (1996a) Age-related changes of α-tocopherol transfer protein expression in rat liver. *J. Nutr. Sci. Vitaminol.* **42**, 11–18.

Kim, J.H., Lingwood, C.A. & Gristein, S. (1996b) Dynamic measurement of the pH of the Golgi complex in living cells using retrograde transport of the verotoxin receptor. *J. Cell Biol.* **134**, 1387–1399.

Kobayashi, T., Stang, E., Fang, K.S., de Moerloose, P., Parton, R.G. & Gruenberg, J. (1998) A lipid associated with the antiphospholipid syndrome regulates endosome structure and function. *Nature* **392**, 193–197.

Krugmann, S., Anderson, K.E., Ridley, S.H., *et al.* (2002) Identification of ARAP3, a novel PI3K effector regulating both Arf and Rho GTPases, by selective capture on phosphoinositide affinity matrices. *Mol. Cell* **9**, 95–108.

Liscum, L. & Dahl, N.K. (1992) Intracellular cholesterol transport. *J. Lipid Res.* **33**, 1239–1254.

Maw, M.A., Kennedy, B., Knight, A., *et al.* (1997) Mutation of the gene encoding cellular retinaldehyde-binding protein in autosomal recessive retinitis pigmentosa. *Nat. Genet.* **17**, 198–200.

Myers, B.M., Prendergast, F.G., Holman, R., Kunts, S.M. & LaRusso, N.F. (1991) Alterations in the structure, physicochemical properties, and pH of hepatocyte lysosomes in experimental iron overload. *J. Clin. Invest.* **88**, 1207–1215.

Nakamura, T. & Kijima, S. (1972) Tocopherol derivatives. IV. Hydroxymethylation reaction of β-, γ-tocopherol and their model compounds with boric acid. *Chem. Pharm. Bull.* **20**, 1681–1686.

Nishikawa, K., Arai, H. & Inoue, K. (1990) Scavenger receptor-mediated uptake and metabolism of lipid vesicles containing acidic phospholipids by mouse peritoneal macrophages. *J. Biol. Chem.* **265**, 5226–5231.

Oram, J.F., Vaughan, A.M. & Stocker, R. (2001) ATP-binding cassette transporter A1 mediates cellular secretion of α-tocopherol. *J. Biol. Chem.* **276**, 39898–39902.

Ouahchi, K., Arita, M., Kayden, H., *et al.* (1995) Ataxia with isolated vitamin E deficiency is caused by mutations in the α-tocopherol transfer protein. *Nat. Genet.* **9**, 141–145.

Saari, J.C., Nawrot, M., Kennedy, B.N., *et al.* (2001) Visual cycle impairment in cellular retinaldehyde binding protein (CRALBP) knockout mice results in delayed dark adaptation. *Neuron* **3**, 739–748.

Sato, Y., Hagiwara, K., Arai, H. & Inoue, K. (1991) Purification and characterization of the α-tocopherol transfer protein from rat liver. *FEBS Lett.* **288**, 41–45.

Sato, Y., Arai, H., Miyata, A., *et al.* (1993) Primary structure of α-tocopherol transfer protein from rat liver. Homology with cellular retinaldehyde-binding protein. *J. Biol. Chem.* **268**, 17705–17710.

Seyer, C.A. & Peters, T.J. (1978) Organelle pathology in primary and secondary haemochromatosis with special reference to lysosomal changes. *Br. J. Haematol.* **40**, 239–253.

Shibata, N., Arita, M., Misaki, Y., *et al.* (2001) Supernatant protein factor, which stimulates the conversion of squalene to lanosterol, is a cytosolic squalene transfer protein and enhances cholesterol biosynthesis. *Proc. Natl. Acad. Sci. USA* **98**, 2244–2249.

Traber, M.G., Ramakrishnan, R. & Kayden, H.J. (1994) Human plasma vitamin E kinetics demonstrate rapid recycling of plasma RRR-alpha-tocopherol. *Proc. Natl. Acad. Sci. USA* **91**, 10005–10008.

Traber, M.G. & Arai, H. (1999) Molecular mechanisms of vitamin E transport. *Annu. Rev. Nutr.* **19**, 343–355.

Watts, C. (1984) *In situ* ^{125}I-labelling of endosome proteins with lactoperoxidase conjugates. *EMBO J.* **3**, 1965–1970.

Wibo, M. & Poole, B. (1974) Protein degradation in cultured cells. II. The uptake of chloroquine by rat fibroblasts and the inhibition of cellular protein degradation and cathepsin B1. *J. Cell Biol.* **63**, 430–440.

Yokota, T., Igarashi, K., Uchihara, T., *et al.* (2001) Delayed-onset ataxia in mice lacking α-tocopherol transfer protein: model for neuronal degeneration caused by chronic oxidative stress. *Proc. Natl. Acad. Sci. USA* **98**, 15185–15190.

Received: 12 June 2003
Accepted: 10 July 2003

THE JOURNAL OF BIOLOGICAL CHEMISTRY
Vol. 279, No. 50, Issue of December 10, pp. 52425–52436, 2004
Printed in U.S.A.

Anti-apoptotic Actions of the Platelet-activating Factor Acetylhydrolase I α_2 Catalytic Subunit*

Received for publication, September 23, 2004
Published, JBC Papers in Press, September 28, 2004, DOI 10.1074/jbc.M410967200

Fanny Bonin‡§¶, Scott D. Ryan‡§, Lamiaa Migahed‡‖, Fan Mo‡‖, Jessica Lallier‡, Doug J. Franks, Hiroyuki Arai‡‡, and Steffany A. L. Bennett‡§§**

*From the ‡Neural Regeneration Laboratory, Department of Biochemistry, Microbiology, and Immunology and the **Department of Pathology, University of Ottawa, Ottawa, Ontario K1H 8M5, Canada and ‡‡Graduate School of Pharmaceutical Sciences, University of Tokyo, 3-1, Hongo-7, Bunkyo-ku, Tokyo 113-0033, Japan*

Platelet-activating factor (PAF) is an important mediator of cell loss following diverse pathophysiological challenges, but the manner in which PAF transduces death is not clear. Both PAF receptor-dependent and -independent pathways are implicated. In this study, we show that extracellular PAF can be internalized through PAF receptor-independent mechanisms and can initiate caspase-3-dependent apoptosis when cytosolic concentrations are elevated by ~15 pM/cell for 60 min. Reducing cytosolic PAF to less than 10 pM/cell terminates apoptotic signaling. By pharmacological inhibition of PAF acetylhydrolase I and II (PAF-AH) activity and down-regulation of PAF-AH I catalytic subunits by RNA interference, we show that the PAF receptor-independent death pathway is regulated by PAF-AH I and, to a lesser extent, by PAF-AH II. Moreover, the anti-apoptotic actions of PAF-AH I are subunit-specific. PAF-AH I α_1 regulates intracellular PAF concentrations under normal physiological conditions, but expression is not sufficient to reduce an acute rise in intracellular PAF levels. PAF-AH I α_2 expression is induced when cells are deprived of serum or exposed to apoptogenic PAF concentrations limiting the duration of pathological cytosolic PAF accumulation. To block PAF receptor-independent death pathway, we screened a panel of PAF antagonists (CV-3988, CV-6209, BN 52021, and FR 49175). BN 52021 and FR 49175 accelerated PAF hydrolysis and inhibited PAF-mediated caspase 3 activation. Both antagonists act indirectly to promote PAF-AH I α_2 homodimer activity by reducing PAF-AH I α_1 expression. These findings identify PAF-AH I α_2 as a potent anti-apoptotic protein and describe a new means of pharmacologically targeting PAF-AH I to inhibit PAF-mediated cell death.

Platelet-activating factor (PAF,[1] 1-*O*-alkyl-2-acetyl-*sn*-glycero-3-phosphocholine) is a key mediator of neuronal death in ischemia, encephalitis, epileptic seizure, meningitis, and human immunodeficiency virus-1 dementia *in vivo* and participates in etoposide-, prion-, and β-amyloid-induced cell death *in vitro* (1–7). In the periphery, pathological increases in PAF concentrations underlie cytotoxicity in chronic inflammatory dermatoses and lethality in systemic anaphylaxis (8, 9). Although the majority of PAF effects are understood to be transduced by its G-protein-coupled receptor (PAFR) (10), PAFR signaling has been shown to be both pro- and anti-apoptotic. Ectopic PAFR expression exacerbates cell death induced by etoposide and mitomycin C but protects cells from tumor necrosis factor α, TRAIL, and extracellular PAF (6, 7, 11, 12). These opposing effects likely depend upon the relative ratio of NF-κB-dependent pro- and anti-apoptotic gene products elicited in different cell types in response to the combination of an external apoptotic inducer and PAF (6).

Accumulating evidence points to additional PAF signaling pathways transduced independently of PAFR (11, 13–17). PAFR-negative cells undergo apoptosis when extracellular PAF concentrations reach 100 nM and necrosis when PAF levels exceed the critical micelle concentration of 3 μM (11). Little is known about how PAF signals cell death in the absence of PAFR. PAF activates NF-κB, glycogen synthase kinase 3β, and caspase 3 and triggers mitochondrial release of cytochrome *c* (6, 18–20). Whether or not these effects are dependent on PAFR activation is not clear.

One approach to intervening in both PAFR-dependent and -independent cell death lies in reducing pathological increases in PAF. PAF is hydrolyzed by a unique family of serine esterases or PAF acetylhydrolases (PAF-AHs) that cleave the biologically *sn*-2 active side chain generating *lyso*-PAF. Three PAF-AH enzymes have been identified. Cytosolic PAF-AH I cleaves the acetyl group at the *sn*-2 position of PAF and PAF-like lipids with other phosphate head groups (21). The enzymatic complex is a G-protein-like trimer composed of two 29-kDa α_1 and α_2 catalytic subunits. The α subunits form homodimers or heterodimers that complex with a noncatalytic 45-kDa regulatory β subunit, LIS1. Mutations in the *LIS1* gene

* This work was supported in part by grants from the Alzheimer Society of Canada, Alzheimer Society of Saskatchewan, and the Canadian Institute of Health Research Joint Initiative (to S. A. L. B.). The costs of publication of this article were defrayed in part by the payment of page charges. This article must therefore be hereby marked "*advertisement*" in accordance with 18 U.S.C. Section 1734 solely to indicate this fact.

The nucleotide sequence(s) reported in this paper has been submitted to the GenBank™/EBI Data Bank with accession number(s) AY225592.

§ Both authors contributed equally to this work.

¶ Supported by a graduate studentship from the Scottish Rite/Roher Foundation.

‖ Supported by a National Research Council undergraduate research award.

§§ Ontario Mental Health Foundation Intermediate Investigator and a Canadian Institute of Health Research New Investigator. To whom correspondence should be addressed: Neural Regeneration Laboratory, Dept. of Biochemistry, Microbiology, and Immunology, University of Ottawa, Ottawa, Ontario K1H 8M5, Canada. Tel.: 613-562-5600 (Ext. 8372); Fax: 613-562-5452; E-mail: sbennet@uottawa.ca.

[1] The abbreviations used are: PAF, platelet-activating factor; B-PAF, Bodipy-platelet-activating factor; B-*lyso*-PAF, Bodipy *lyso*-PAF; BSA, bovine serum albumin; GAPDH, glyceraldehyde-3-phosphate dehydrogenase; DFP, diisopropyl fluorophosphate; DTNB, 5,5prime-dithiobis(2-nitrobenzoic acid; mc-PAF, methyl-carbamyl platelet-activating factor; PAF-AH, PAF acetylhydrolase; PAFR, platelet-activating factor receptor; PARP, poly(ADP-ribose) polymerase; PBS, phosphate-buffered saline; siRNA, small interfering RNA; RT, reverse transcription; TUNEL, terminal deoxytransferase dUTP nick-end labeling; ANOVA, analysis of variance; EGFP, enhanced green fluorescent protein.

are the genetic determinant of Miller-Dieker syndrome, a developmental brain disorder defined by type 1 lissencephaly (22). PAF-AH II is a single 40-kDa polypeptide (23). This isoenzyme recognizes both PAF and acyl analogs of PAF with moderate length *sn*-2 chains as well as short chain diacylglycerols, triacylglycerols, and acetylated alkanols (24). Ectopic expression reduces cell death triggered by oxidative stress (25, 26). Plasma PAF-AH is a 45-kDa monomer secreted into circulation by endothelial and hematopoietic cells (27, 28). The enzyme recognizes PAF and PAF analogs with short to medium *sn*-2 chains including oxidatively cleaved long chain polyunsaturated acyl chains (24). *In vitro*, recombinant plasma PAF-AH or ectopic expression protects cells from excitotoxicity or hypercholesterolemia (29–31). *In vivo*, intravenous injection of human plasma PAF-AH reduces lethality in experimental models of anaphylactic shock (8). These findings provide compelling evidence that PAF-AH activity regulates PAF-mediated apoptosis. It remains to be determined whether these enzymes can, in fact, be targeted to inhibit PAF-mediated degeneration and disease.

In this study, we used the PC12 cell model to investigate the anti-apoptotic actions of PAF-AH I and PAF-AH II in the PAFR-independent death pathway. We show that PC12 cells express all three PAF-AH I proteins (α_1, α_2, and LIS1) as well as PAF-AH II but not plasma PAF-AH or PAFR. Expression of PAF-AH I α_2 but not PAF-AH I α_1 is induced when PC12 cells are deprived of serum. We found that this induction regulates the duration of apoptotic signaling initiated by PAF challenge. To enhance the endogenous anti-apoptotic activity of PAF-AH I α_2, we screened a panel of PAF antagonists, and we identified two compounds that blocked PAFR-independent death. Both compounds, the fungal derivative FR 49175 and the ginkgolide BN 52021, protected cells by accelerating PAF hydrolysis. Most surprisingly, both inhibitors suppressed α_1 protein expression thereby promoting α_2/α_2 homodimer activity following PAF treatment. These findings point to a novel anti-apoptotic function for the α_2 subunit of PAF-AH I and a potential means of pharmacologically targeting PAF-AH enzymes to reduce PAF-mediated cell death.

EXPERIMENTAL PROCEDURES

Cell Culture—PC12-AC cells, a clonal derivative of the PC12 pheochromocytoma cell line (American Tissue Culture Collection), were cultured in complete media composed of RPMI 1640 containing 10% horse serum and 5% newborn calf serum at 37 °C in a 5% CO_2, 95% air atmosphere. Culture reagents were obtained from Invitrogen.

Reverse Transcriptase (RT)-PCR—Rat brain RNA was prepared from Wistar rats ~3 months of age (Charles River Breeding Laboratories). Rodents were anesthetized with sodium pentobarbital and euthanized by decapitation. All manipulations were performed in compliance with approved institutional protocols and according to the strict ethical guidelines for animal experimentation established by the Canadian Council for Animal Care. Total RNA was isolated using Trizol reagent (Invitrogen) and treated with RQ1-DNase I (Promega) to eliminate residual genomic DNA. First strand cDNA synthesis was performed using random hexamer primers (Promega) and Superscript II RT (Invitrogen). Control reactions for residual genomic contamination were carried out in the absence of Superscript II RT. cDNA synthesis was performed using 5 units of *Taq* DNA polymerase (Invitrogen) in the presence of 1 mM $MgCl_2$ and 10 pmol per primer for glyceraldehyde phosphate dehydrogenase (GAPDH), 20 pmol per primer for PAF-AH II2, PAF-AH II3, and PAF-AH II4, and 25 pmol per primer for PAF-AH I α_1, PAF-AH I α_2, PAF-AH I LIS1, PAF-AH II1, plasma PAF-AH, and PAFR. Sequences are provided in Table I. Primers were synthesized at the Biochemistry Research Institute, University of Ottawa. Reactions were amplified in a GeneAmp PCR System 2400 (Applied Biosystems): 94 °C for 5 min, 30–35 cycles of 94 °C for 30 s, 55 °C for 60 s, and 72 °C for 2 min, followed by a final incubation at 72 °C for 7 min.

Western Analysis—Rat brain protein was prepared from Wistar rat pups on postnatal day 10. Rodents were anesthetized with sodium pentobarbital and euthanized by decapitation. Brains were removed and placed in a 10-cm tissue culture plate containing artificial cerebrospinal fluid (26 mM $NaHCO_3$, 124 mM NaCl, 5 mM KCl, 2 mM $CaCl_2$, 1.3 mM $MgCl_2$, 10 mM D-glucose, 100 units/ml penicillin, 100 μg/ml streptomycin, pH 7.3) and homogenized using a Tissue Tearor (Fisher). Protein was isolated using Trizol reagent (Invitrogen). Proteins from PC12 cells were isolated in RIPA buffer (10 mM PBS, 1% Nonidet P-40, 0.5% sodium deoxycholate, 0.1% SDS, 30 μl/ml aprotinin, 10 mM sodium orthovanadate, 100 μl/ml phenylmethylsulfonyl fluoride). Protein samples (30 μg) were separated by SDS-PAGE under reducing conditions. Antibodies were diluted in 1% heat-denaturated casein in 10 mM phosphate-buffered saline (PBS: 10 mM sodium phosphate, 2.7 mM KCl, 4.3 mM NaCl, pH 7.5). Western analyses were performed using polyclonal anti-LIS1 (1:500, Chemicon), monoclonal anti-α_1 (1:1000, Dr. H. Arai, University of Tokyo, Tokyo, Japan), monoclonal anti-α_2 (1:1000, Dr. H. Arai), poly(ADP-ribose) polymerase (PARP, 1:10, 000, Clontech), and actin (1:1000, Sigma). Secondary antibodies were horseradish peroxidase-conjugated or biotin-conjugated anti-mouse IgG (1:2000, Jackson ImmunoResearch; 1:10, 000, Sigma) or anti-rabbit IgG antibodies (1:5000, Jackson ImmunoResearch), and tertiary reagents were extravidin alkaline phosphatase (1:300,000, Sigma) as appropriate. Immunoreactive bands were visualized using SuperSignal West Pico (MJS BioLynx Inc.) or nitro blue tetrazolium/5-bromo-4-chloro-3-indolyl phosphate (Sigma). Densitometry was performed using ImageJ analysis software (National Institutes of Health) standardized to actin loading controls.

PAF-AH Activity—PAF-AH activities in complete media, serum-free RPMI, PC12-AC cells, PC12-AC conditioned treatment media, and C57Bl/6 mouse brain ~3 months of age (positive control) were determined using a commercial PAF-AH assay kit (Cayman Chemicals). Cells and tissue were homogenized in 250 mM sucrose, 10 mM Tris-HCl (pH 7.4), and 1 mM EDTA using a Tissue Tearor (Fisher). Samples were centrifuged at 600 × *g* for 10 min and at 100,000 × *g* for 60 min. Cytosolic supernatants were concentrated using an Amicon centrifuge concentrator with a molecular mass cut-off of 10,000 kDa (Millipore). Protein (30–50 μg) was incubated with C_{16}-2-thio-PAF substrate for 30 min at room temperature. In some cases, lysates were pretreated for 15 or 30 min at room temperature with diisopropyl fluorophosphate (DFP) at the concentrations indicated in the text. Percent inhibition was calculated relative to lysates treated with vehicle (PBS) for the same time. Hydrolysis of the thioester bond at the *sn*-2 position was detected by conjugation with 5,5′-dithiobis(2-nitrobenzoic acid) (DTNB) at 405 nM. Control reactions included samples incubated without lysate or media and samples incubated without substrate.

Internalization Assay (Live Cell Imaging)—PC12-AC cells (5 × 10^4 cells/well) were plated in complete media overnight in 24-well plates (VWR Scientific) coated with 0.1% gelatin. Cells were washed in 10 mM PBS and incubated with 1 μM Bodipy FL C_{11}-PAF (B-PAF) in RPMI 1640 containing 0.1% bovine serum albumin (BSA, Sigma). B-PAF was custom-synthesized for our laboratory by Molecular Probes. At each time point (0, 10, 20, 30, 40, 50, 60, 80, 90, 100, 110, and 120 min), incubation media were removed, and cells were washed with 10 mM PBS. Live cell imaging under phase and fluorescence of identical cell fields was performed using a DMR inverted microscope (Leica) equipped with a QICAM digital camera (Quorum Technologies) and captured using OpenLab software version 3.17 (Improvision). Following time-lapse imaging, the incubation media were replaced, and internalization was allowed to continue. Quantitation of fluorescence intensity of individual cells was performed using the Advanced Measurement Module of OpenLab version 3.17.

Lipid Extraction and TLC—PC12-AC cells seeded at 1 × 10^6 cells onto 10-cm plates were maintained in complete media at 37 °C in 5% CO_2 for 72 h. Cultures were incubated at 37 °C with 1 μM B-PAF in RPMI 1640 containing 0.1% BSA for 0, 5, 15, 30, 45, 60, and 75 min. At each time point, 4 plates/condition were removed from the incubator and were placed on ice. One ml of methanol acidified with 2% acetic acid was added to each plate, and the extracellular fraction was collected. This fraction contained B-PAF in the culture media and uninternalized B-PAF bound to cell surface proteins or associated with the plasma membrane. The remaining monolayer of cells was collected in acidified methanol by scraping the plate with a cell lifter (Fisher). Lipids were extracted from the extracellular milieu and cytosolic fractions by the Bligh and Dyer method (32) and developed on TLC plates (20 × 20 cm Silica Gel 60 (Fisher) in a solvent system of chloroform/methanol/acetic acid/water (50:30:8:5, v/v). B-PAF and B-*lyso*-PAF (Molecular Probes) were used as authentic markers. Fluorescent lipids were visualized under UV light using AlphaImager-1220 software (Alpha Innotech Corp.). Fluorescence intensity corresponding to lipid yield was determined by densitometry using the Advanced Measurement Module of

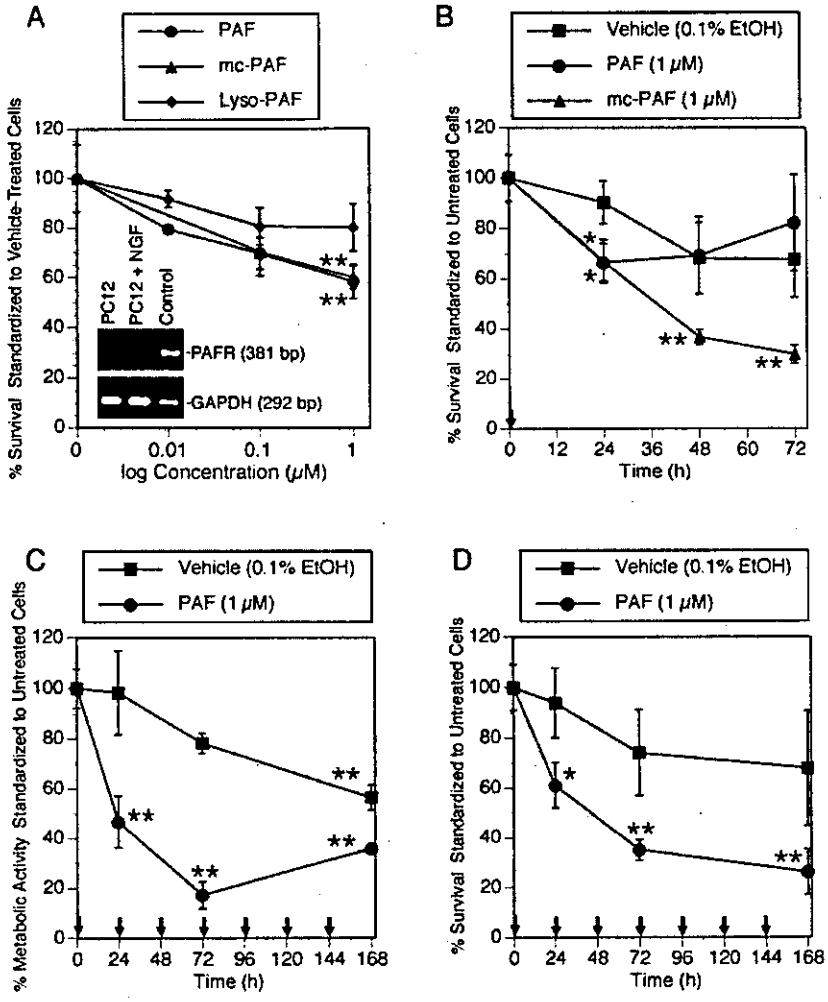

FIG. 1. **The kinetics of PAF-mediated apoptosis initiated independently of PAFR depend upon sustained exposure to active ligand.** *A*, PC12-AC cells were treated for 24 h with PAF (0.01–1 μM), mc-PAF (0.01–1 μM), or *lyso*-PAF (0.01–1 μM) in serum-free treatment media. A dose-dependent decrease in cell number relative vehicle (0.1% EtOH)-treated cells was observed after 24 h of treatment with 1 μM PAF or mc-PAF (**, $p < 0.01$). RT-PCR analysis of PC12-AC cultures (*inset*) confirmed that both PC12-AC cells (*PC12*) and PC12-AC cells differentiated to a neuronal phenotype for 7 days with nerve growth factor (*PC12+NGF*) do not express PAFR mRNA. The positive control was RNA isolated from PC12 cells stably transfected with PAFR. cDNA template integrity was confirmed using GAPDH as an internal standard (*GAPDH*). *B*, PAF (1 μM) treatment resulted in significant cell loss within 24 h of treatment (*, $p < 0.05$) after which no additional reductions in cell number were observed. mc-PAF (1 μM) elicited incremental cell loss for up to 48 h after exposure (*, $p < 0.05$; **, $p < 0.01$). Culture in serum-free treatment media in the presence of vehicle (EtOH, 0.1%) did not affect cell viability until 48 h after treatment. *Arrows* indicate the time of PAF administration. *C*, repeated PAF (1 μM) administration incrementally decreased the metabolic activity of cells for up to 72 h as defined by the ability of mitochondrial dehydrogenases to reduce the formazan salt WST (**, $p < 0.01$). *Arrows* indicate the time when PAF (1 μM) or vehicle (0.1% EtOH) was replenished in fresh media. *D*, incremental cell loss was observed for up to 48 h following chronic PAF (1 μM) treatment. (*, $p < 0.05$; **, $p < 0.01$, ANOVA, post-*hoc* Dunnett's *t* test). As in *C*, media were replaced, and PAF (1 μM) or vehicle (0.1% EtOH) was added every 24 h (*arrows*). *A*, data are expressed as percent survival of vehicle-treated cultures. *B–D*, the data are standardized to untreated cells cultured in treatment media to present the effect of vehicle treatment on cell survival. Results are reported as mean ± S.E. of $n = 5–26$ cultures per data point.

OpenLab version 3.17. Concentrations of cytosolic B-PAF were estimated in comparison to a B-PAF standard curve resolved in parallel. Data are expressed as pM/PAF-responsive cell following standardization to the number of cells/culture.

Cell Death Assays—PC12-AC cells (8800 cells/cm^2) were plated overnight in complete media in 6-cm diameter tissue culture plates (VWR Scientific). Cells were treated in serum-free RPMI media containing 0.025% BSA (treatment media) for 24–72 h with EtOH (0.1%), PAF (10 nM-1 μM, Biomol Research Laboratories), methyl-carbamyl-PAF (mc-PAF; 100 nM-1 μM, Biomol Research Laboratories), or *lyso*-PAF (10 nM-1 μM, Biomol Research Laboratories). In some cases, cells were pretreated with BN 52021 (1–100 μM, Biomol Research Laboratories), CV-3988 (0.2–2 μM, Biomol Research Laboratories), CV-6209 (1–10 μM, Biomol Research Laboratories), FR 49175 (0.5–50 μM, Biomol Research Laboratories), DFP (0.1 mM or 1 mM, Sigma), DTNB (1 mM, Sigma), or combinations thereof for 15 min followed by addition of PAF (1 μM) for 24 h. Cell survival was assessed by hemocytometer cell counts of trypan blue-excluding cells. Metabolic activity was assessed based on the ability of mitochondrial dehydrogenases, active in viable cells, to reduce the formazan salt, WST-1 (measured at A_{450}–$A_{690\ nm}$, Roche Applied Science). DNA fragmentation was determined by terminal deoxytransferase dUTP nick-end labeling (TUNEL, Roche Applied Science) of cultures fixed for 20 min in 4% paraformaldehyde in 10 mM as described previously (33). Cells, processed for TUNEL, were double-labeled with Hoechst 33258 (0.2 μg/ml) for 20 min at room temperature for additional morphological evidence of apoptotic loss.

RNA Interference Transfection—To suppress expression of the PAF-AH I α_2 subunit, we designed a double-stranded short interfering RNA (siRNA) to the α_2 sequence (AATAAACATGCTTGTCACTCCC/CTGTCTC) and a negative control scrambled sequence (AATGCATAGGAGTTGGAGAGGC/CTGTCTC). Oligonucleotides were obtained from the Biotechnology Research Institute at the University of Ottawa. siRNA duplexes were generated using the Silencer siRNA construction kit (Ambion). Transfection of siRNA was performed with LipofectAMINE 2000 (Invitrogen) and optimized to yield maximal transfection efficiency according to manufacturer's protocol. Briefly, 2 μl of LipofectAMINE 2000 was diluted in 198 μl of RPMI 1640 media for 5 min at room temperature. siRNA duplexes (PAF-AH α_2 or scrambled) were suspended in 100 μl of RPMI 1640 media. PC12-AC cells grown in complete media to 30% confluence in 4-well gelatin-coated Labtek wells were treated with 100 μl of the LipofectAMINE-siRNA complex and incubated for 72 h at 37 °C. Transfection efficiency was determined in

separate cultures by counting EGFP-positive cells upon transfection with pEGFP-C1 as well as morphological changes using β-actin siRNA positive control (Ambion). Because we were unable to obtain >20% transfection efficiency, we co-transfected PAF-AH α_2 or scrambled siRNAs with 0.028 μg/μl of pEGFP-C1 to identify silenced cells. Cells were then exposed to 1 μM PAF in treatment media (RPMI + 0.025% BSA) for either 45 min or 24 h. Data were standardized to the number of EGFP-positive cells in vehicle-treated cultures transfected with pEGFP-C1 only.

Statistical Analysis—Data were analyzed by using ANOVA tests or unpaired Student's *t* tests, as applicable. Following detection of a statistically significant difference in a given series of treatments, *post hoc* Dunnett's *t*-tests or Tukey tests were performed where appropriate. *p* values under 0.05 were considered statistically significant (shown as * or †); *p* values under 0.01 were considered highly statistically significant (shown as ** or ††).

RESULTS

PAF Can Elicit Apoptosis Independently of Its G-protein-coupled Receptor—We have demonstrated previously (11) that PC12-AC cells do not express PAFR but undergo apoptosis-associated DNA fragmentation 24 h after treatment with ≥100 nM PAF and necrotic lysis when treated with >3 μM PAF. In this study, we addressed the kinetics and underlying signaling mechanism of PAF-induced apoptosis in the absence of PAFR (Fig. 1*A*, *inset*). To determine whether cell death is mediated by PAF or downstream PAF metabolites, PC12-AC cells were treated with PAF, mc-PAF, the PAF-AH-resistant synthetic PAF analog (34), or *lyso*-PAF, the immediate PAF metabolite. Both mc-PAF and PAF triggered comparable concentration-dependent cell death 24 h after treatment (Fig. 1*A*). *lyso*-PAF had no significant effect on cell viability (Fig. 1*A*). To establish the kinetics of PAF-mediated cytotoxicity, cell survival was assessed at various times after phospholipid administration. PAF (1 μM) elicited significant cell loss within 24 h of treatment; no further reductions in cell number were detected at 48 or 72 h relative to vehicle controls (Fig. 1*B*). mc-PAF (1 μM) elicited incremental cell loss for up to 72 after treatment (Fig. 1*B*). Comparable kinetics were observed if PAF (1 μM) was replenished in fresh media at 24-h intervals with cells repeatedly treated with PAF exhibiting sustained impairment of cellular metabolic activity (Fig. 1*C*) and an incremental reduction in cell survival (Fig. 1*D*).

To determine whether PAF activates caspases in the absence of PAFR, we examined cleavage of the caspase 3 substrate PARP. Caspase 3-mediated PARP cleavage from 116 to 85 kDa was observed 45 min after a single PAF treatment (Fig. 2*A*). Cleavage markedly increased 3 h after phospholipid administration and was detected for up to 24 h after treatment (Fig. 2*A*) but not at later time points (data not shown). TUNEL-positive cells, evidence of terminal DNA fragmentation, were first observed 24 h after PAF exposure with no evidence of additional death 48 h after exposure (Fig. 2*B*).

Collectively, these findings indicate the following. (*a*) PAF can activate caspase 3 independently of its G-protein-coupled receptor within 45 min of treatment. (*b*) This PAFR-independent apoptotic pathway culminates in terminal DNA fragmentation 24 h after treatment. (*c*) Cell death is not mediated by downstream metabolites. (*d*) Incremental cell death depends upon repeated exposure to active ligand or treatment with PAF-AH-resistant PAF analogs.

Cytosolic PAF-AH Enzymes Limit the Duration of PAF-induced Apoptotic Signaling—These kinetics implicate PAF degradation in the control of apoptotic signaling. To test this hypothesis, we first identified *LIS1*, PAF-AH I α_1, PAH-AH I α_2, and PAF-AH II but not plasma PAF-AH transcripts in PC12 cells by RT-PCR (Fig. 3, *A–F*). Amplicon integrity of the PAF-AH I subunits was verified by sequencing on both strands. We then confirmed protein expression by Western analysis. α_1

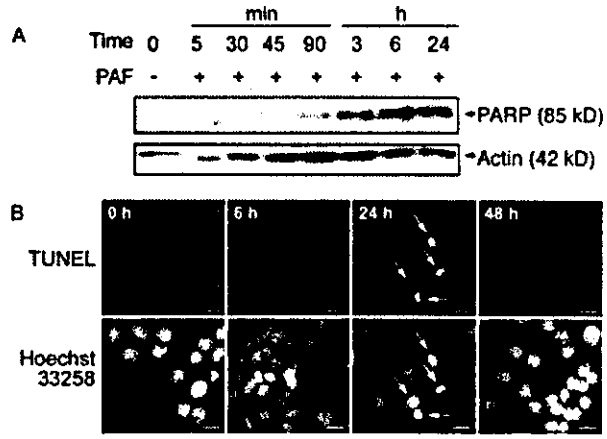

FIG. 2. **PAF triggers a caspase-dependent apoptotic cascade within 45 min of exposure to active ligand.** *A*, PC12-AC cells were exposed to PAF (1 μM) for 24 h and assayed for caspase 3 activity. PARP cleavage to 85 kDa was first detected 45 min after PAF treatment. Blots were re-probed with actin as a loading control. *B*, TUNEL analysis detected apoptosis-associated DNA cleavage (*arrows, upper panel*) and DNA condensation (*arrows, lower panel*) 24 h after PAF treatment. No additional cell loss was observed 48 h after treatment. *Scale bar*, 10 μm.

protein was constitutively expressed in the presence or absence of PAF (Fig. 3*G*). α_2 protein was present at extremely low levels (Fig. 3, *H* and *I*) with marked induction following exposure to PAF (Fig. 3, *H* and *I*). Closer examination revealed that α_2 protein also increased when cells were cultured in serum-free treatment media suggesting a response to serum withdrawal rather than PAF-specific induction (Fig. 3*I*). LIS1 was constitutively expressed by PC12-AC cells (Fig. 3*J*).

Lacking an antibody to PAF-AH II to verify protein expression, we sequenced the full-length transcript and assayed functional PAF-AH activity in the presence of cytosolic PAF-AH I and II inhibitors. Full-length transcript was amplified from Wistar rat brain and PC12-AC cells using a series of primer pairs homologous to conserved sequences in murine, bovine, and human genes (Table I). A 1173-bp open reading frame was identified in both PC12-AC cells and Wistar rat brain with no base pair mismatches between the sequences.[2] In functional assays, total cytosolic PAF-AH activity in cell lysates was comparable with enzymatic activity in adult mouse brain homogenates (Table II). PAF hydrolytic activity was not detected in treatment media harvested from cells after 24 h of culture confirming the RT-PCR analysis that PC12-AC cells do not express the secreted PAF-AH isoenzyme (Table II). To distinguish between PAF-AH I and PAF-AH II activity, cell lysates were treated with the active serine blocking agent DFP. 0.1 mM DFP inhibits PAF-AH I α_1/α_1 or α_1/α_2 dimer activity, whereas 1 mM DFP inhibits PAF-AH I α_1/α_1, PAF-AH I α_1/α_2, and PAF-AH II activity. PAF-AH I α_2/α_2 dimers are DFP-resistant (21, 23, 35). 68–70% of the total cytosolic PAF-AH activity was blocked by 0.1 mM DFP indicative of PAFAH I α_1/α_1 or α_1/α_2 activity (Table II). Increasing the DFP concentration to 1 mM blocked an additional 4–7% of PAF-AH activity attributed to PAF-AH II. DFP-resistant PAF-AH I α_2/α_2 homodimer activity composed 25% of cytosolic PAF-AH activity in lysates extracted from cells cultured in complete media.

The kinetics of PAF hydrolysis by PAF-AH I and II were established using the fluorescent PAF substrate B-PAF. Cells were treated with 1 μM B-PAF to initiate apoptotic signaling. B-PAF and its metabolites were extracted at various time points using a modified Bligh and Dyer procedure and identi-

[2] The rat PAF-AH II cDNA cloned from adult Wistar rat brain was deposited under GenBank™ accession number AY225592.

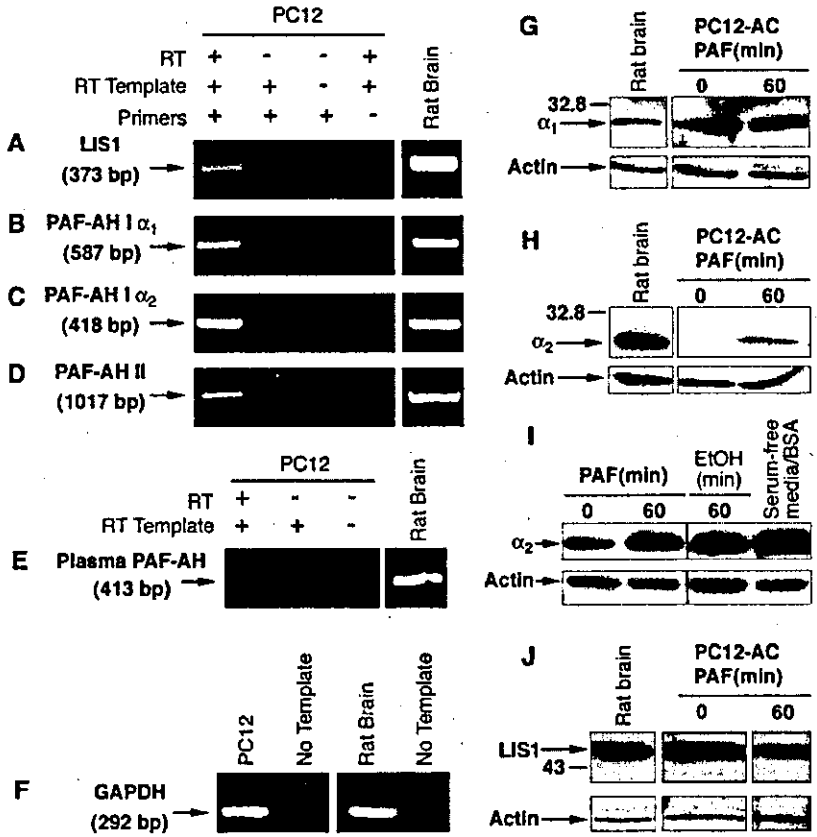

FIG. 3. **Expression patterns of PAF-AH I, PAF-AH II, and plasma PAF-AH in PC12-AC cells.** RT-PCR was performed for LIS1 (*A*), PAF-AH I α_1 (*B*), PAF-AH I α_2 (*C*), and PAF-AH II (*D*). Plasma PAF-AH mRNA was not detected (*E*). The absence of genomic DNA contamination or reagent contamination was confirmed by the control reactions: no RT during the RT reaction, no template during the PCR reaction, and no primers during the PCR reaction. Rat brain RNA was reverse-transcribed as a same-species positive control (*Rat Brain lane*). Template integrity of the random-primed PC12-AC RT product was verified by using GAPDH (*F*). Equal amounts of protein (30 μg) from cells cultured in complete media (*0*) or cells treated for 60 min with 1 μM PAF in treatment media (*60*) were separated under reducing conditions and immunoblotted for α_1 (*G*), α_2 (*H* and *I*), or LIS1 (*J*). Protein lysates from neonatal rat brain were used as a same-species positive control. Representative immunoblots of replicate experiments are depicted. PAF-AH α_1 was constitutively expressed (*G*). Significant PAF-AH α_2 protein was not detected until cells were treated with PAF (1 μM) (*H*). Longer exposure times (overnight) indicated that PC12-AC cells expressed low levels of protein and that serum deprivation was sufficient to induce α_2 protein expression (*I*). LIS1 was constitutively expressed (*J*). Blots were probed for actin as a loading control (*G–J*).

TABLE I
Primer pairs used to detect cytosolic and plasma PAF-AH transcript by RT-PCR

Gene	Strand	Sequence (5′–3′)	Amplicon size
			bp
GAPDH	Sense	TGGTGCTGAGTATGTCGTGGAGT	292
	Antisense	AGTCTTCTGAGTGGCAGTGATGG	
PAF-AH I α_1	Sense	GACGGACGCTGGATGTCTCT	587
	Antisense	AGACGAAGCAGCAAGGAGTG	
PAF-AH I α_2	Sense	TGCAGCAGTACGAGATATGG	418
	Antisense	AACATGTCGTGGCAGGAGAT	
PAF-AH I LIS1	Sense	CTGCTTCAGAGGATGCTACA	373
	Antisense	ATCAGAGTGCCGTCCTGATT	
PAF-AH II1	Sense	GGATGTGATGGAGGGTC	1017
	Antisense	TGCTTCTGCAGGAAGGCCAA	
PAF-AH II2	Sense	CAGCTGGTGATGAGATGG	224
	Antisense	GCGCTTGTTATACTGCAGGT	
PAF-AH II3	Sense	TGAGCCGAGTGGCTGTGATG	472
	Antisense	CCCTTGGATGAGCGATGGTC	
PAF-AH II4	Sense	CAGCTGGTGATGAGATGG	1250
	Antisense	CAACCTAGAGGCTGGACAGA	
Plasma PAF-AH	Sense	GGGGCATTCTTTTGGAGGAG	413
	Antisense	GACAGTCCCACTGATCAAAGTC	
PAFR	Sense	CACTTATAACCGCTACCAGGCAG	381
	Antisense	AAGACAGTGCAGACCATCCACAG	

fied by TLC. Fluorescent intensity was quantified by comparison to resolved fluorescent standards. Cytosolic and extracellular lipids were fractionated from B-PAF-treated cultures with an acidified methanol wash separating phospholipids bound to proteins on plasma membrane from internalized lipids (36). We found that 1 μM B-PAF was stable in cell-free, serum-free treatment media at 37 °C for at least 60 min; no degradation to B-*lyso*-PAF was observed in the absence of cells (Fig. 4*A*). B-PAF was rapidly internalized by PC12-AC cells (Fig. 4*B*, *extracellular*) with concentrations reaching ~16–20

TABLE II
PAF-AH activity in PC12-AC cells, mouse brain lysate, and tissue culture media

PAF-AH activity[a]							
Mouse brain lysate, positive control	PC12-AC lysates				Cell-free media		
	Untreated lysates	% inhibition[b]					
		Time	0.1 mM DFP	1 mM DFP	Complete media	Serum-free treatment media	PC12-AC-conditioned treatment media
	nmol/min/μg or % inhibition	*min*	*nmol/min/μg or % inhibition*			*nmol/min/μg or % inhibition*	
1.97 ± 0.44 $n = 8$	1.37 ± 0.19 $n = 23$	15	68% $n = 6$	75% $n = 5$	3.36 ± 0.10 $n = 2$	0.01 ± 0.00 $n = 2$	0.00 ± 0.00 $n = 3$
		30	70% $n = 3$	74% $n = 3$			

[a] Data represent mean ± S.E. n denotes the number of replicates conducted over 1–4 experiments.
[b] Lysates were pretreated for 15 or 30 min at room temperature with vehicle (10 mM PBS) or the indicated concentrations of DFP. Activity in vehicle-treated cultures was equivalent to that detected in untreated cultures. % inhibition was determined as described under "Materials and Methods."

pM/cell within 5 min of incubation (Fig. 4*B*, *cytosolic*). Internalized B-PAF levels remained constant for 60 min dropping to 6–8 pM/cell by 75 min (Fig. 4*B*, *cytosolic*). B-PAF degradation was detected within 15 min of internalization (Fig. 4*C*, *vehicle*). A linear rate of metabolism ($r^2 = 0.97$) was observed for up to 75 min (Fig. 4*C*, *vehicle*). Closer examination of the fate of B-PAF metabolite by fractionation revealed that B-*lyso*-PAF was released from cells in two stages (Fig. 4*D*). Between 5 and 15 min of incubation, 50% of internalized B-PAF was converted to B-*lyso*-PAF (Fig. 4*D*, *Cytosolic*) and secreted from the cells (Fig. 4*D*, *extracellular*). Between 30 and 60 min, B-*lyso*-PAF was not released and accumulated in the cell cytosol (Fig. 4*D*, *cytosolic*). A delayed phase of secretion was observed between 60 and 75 min (Fig. 4*D*, *extracellular*).

To track the fate of secreted B-*lyso*-PAF, we performed quantitative time-lapse fluorescence microscopy (Fig. 4*E*). B-PAF-containing media were removed, and cells were washed with PBS containing 1% BSA at various time points to remove free lipids loosely associated with the plasma membrane but not phospholipids bound to membrane proteins. Cells were photographed, and the B-PAF-containing media were replaced. A linear increase in cell-associated fluorescence was observed over the first 70 min of exposure ($r^2 = 0.97$) followed by a plateau in cell-associated B-PAF (Fig. 4*E*).

Taken together, these data indicate that PAF administered to cells is metabolized by PAF-AH I and II with a $t_{1/2}$ of 75 min (where $t_{1/2}$ is the time to reach half-maximal concentrations). The PAF metabolite, *lyso*-PAF, is secreted from cells but remains bound, apparently to carrier proteins, on the extracellular surface of the plasma membrane.

Cytosolic PAF-AHs Can Be Targeted Pharmacologically to Promote Cell Survival—The kinetics of PAF-induced apoptosis (Figs. 1 and 2) and PAF degradation (Fig. 4) suggest that cytosolic PAF concentrations must remain elevated for at least 60 min to elicit apoptosis. This hypothesis predicts that compounds capable of inhibiting PAF internalization or increasing cytosolic PAF-AH activity will block PAF-mediated death triggered independently of PAFR. To test this hypothesis, we evaluated the anti-apoptotic actions of four PAF antagonists (CV-3988, CV-6209, BN 52021, and FR 49175). These compounds were chosen because of their affinities for different PAF-binding sites identified pharmacologically. CV-3988 and CV-6209 are competitive PAF antagonists that preferentially interact with synaptosomal and microsomal PAF-binding sites (17). CV-3988 competes for PAF at the plasma membrane, likely PAFR, as well as interacting with intracellular microsomal binding sites, likely internalized PAFR (17). CV-6209 preferentially interacts with a single binding site in microsomal membranes (17). BN 52021 (also known as ginkgolide B) is a noncompetitive PAF antagonist with affinity for three discrete PAF-binding sites (17) as well as potent antioxidant activity (37). FR 49175 is a fungal metabolite derivative that inhibits PAF-induced biological activity through unknown mechanisms (38, 39). Treatment of PC12-AC cells with CV-3988, BN 52021, or FR 49175 had no effect on cell survival (Fig. 5, *A–C*); however, CV-6209 was toxic to cells at concentrations above 1 μM (Fig. 5*D*). We observed significant concentration-dependent anti-apoptotic activity when cells were preincubated for 15 min with BN 52021 (1–100 μM) or FR 49175 (0.5–50 μM) and then exposed to PAF (Fig. 5*E*). Both BN 52021 and FR 49175 inhibited PAF-mediated caspase 3 activation as assessed by PARP cleavage (Fig. 5*F*). CV-3988 (0.1–10 μM) and CV-6209 (0.01–1 μM) did not exhibit anti-apoptotic activity (Fig. 5*E*).

We next tracked B-PAF fate by lipid extraction and TLC in the presence or absence of BN 52021 and FR 49175 to establish whether these antagonists affect phospholipid internalization or PAF-AH activity. FR 49175 and BN 52021 did not alter the rate or extent of B-PAF internalization (Fig. 6, *A* and *D*, *extracellular*). In both antagonist- and vehicle-treated cultures, maximal cytosolic B-PAF levels were attained within 5 min of B-PAF exposure (Fig. 6, *A* and *D*, *cytosolic 5 min*). We did not observe an increase in total B-PAF hydrolysis. Cytosolic B-PAF concentrations, estimated at 8 pM/cell, in BN 52021- and FR 49175-treated cultures were comparable with vehicle-treated cells by the end of the 75 min test period (Fig. 6, *A* and *D*, *cytosolic, 75 min*). Significantly, we found that FR 49175 and BN 52021 accelerated both the kinetics of B-PAF degradation (Fig. 6, *A* and *D*, *45 min*) and the release of B-*lyso*-PAF into the media (compare Fig. 6, *B* and *E*, *cytosolic 45 min* and *C* and *F*, *extracellular, 45 min*). By 45 min, 39 (FR 49175) or 41% (BN 52021) of exogenous B-PAF had been converted to B-*lyso*-PAF compared with 29% in vehicle-treated cells. This acceleration dropped cytosolic B-PAF levels more rapidly in antagonist-treated cultures from 16 pM/cell (5 min) to 10 pM/cell (45 min) in the presence of FR 49175 or 8 pM/cell (45 min) in the presence of BN 52021 (Fig. 6, *B* and *E*). Maximal release of B-*lyso*-PAF from cells was observed within 45 min in antagonist-treated cultures compared with 75 min in vehicle-treated cultures (Fig. 6, *C* and *F*). 50% of the released metabolite diffused or was transported back into the cells within 75 min in FR 49175 treated cultures; 32% of B-*lyso*-PAF re-entered cells in BN 52021-treated cultures (Fig. 6, *B–F*).

PAF-AH I α_2/α_2 Activity Is Anti-apoptotic—To determine how BN 52021 and FR 49175 accelerate PAF-AH hydrolysis, we examined PAF-AH I α_1 and α_2 expression. Cells were preincubated in serum-free treatment media with vehicle (Me_2SO), BN 52021, or FR 49175 for 15 min before addition of PAF (Fig. 7). We found PAF-AH α_1 expression remained constant whether cells were cultured in complete media, serum-free treatment media, pretreated with Me_2SO, or exposed to PAF (Fig. 7*A*,

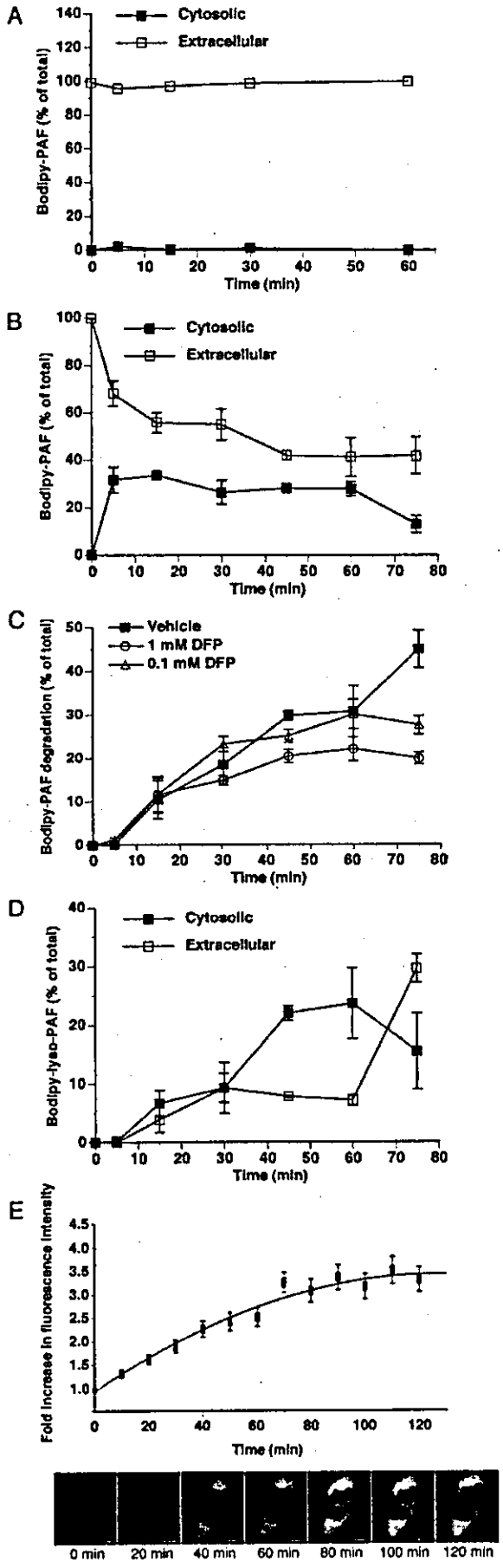

FIG. 4. **Internalization, kinetic analysis, and metabolic fate of B-PAF and B-*lyso*-PAF in PC12-AC cells.** PC12 cells were incubated with 1 μM B-PAF at 37 °C for 0, 5, 15, 30, 45, 60, and 75 min. At each time point, lipids were extracted from the extracellular and cytosolic fractions and were separated by TLC. *A–C*, data represent relative fluorescence of B-PAF in each fraction expressed as a percentage of the total fluorescent lipids recovered. Data are the mean of 2–4 independent experiments conducted in replicate. *A*, B-PAF was not degraded by treatment media in the absence of PC12 cells. *B*, in cell cultures, B-PAF was rapidly internalized within 5 min (*extracellular fraction*) after which levels remained stable until 60 min and dropped by 75 min (*cytosolic fraction*). *C*, conversion of B-PAF to B-*lyso*-PAF was monitored to determine the degree of PAF hydrolysis in the presence or absence of the PAF-AH I α_1 and PAF-AH II inhibitor DFP. Cells were pretreated for 15 min in treatment media with vehicle (PBS) or DFP before addition of B-PAF. *D*, the fate of the B-PAF metabolite B-*lyso*-PAF was followed by fractionation. *E*, to determine whether B-*lyso*-PAF secreted from cells remains loosely associated with the lipid bilayer or bound to membrane proteins, cell-associated fluorescence was tracked by live-cell imaging. The B-PAF containing media were removed every 10 min, and cells were washed with PBS + 1% BSA to remove phospholipids at the extracellular face of the plasma membrane but not lipids associated with membrane proteins. Data are reported as the mean increase in fluorescence intensity standardized to background fluorescence in untreated cells ± S.E. (n = 16–25 per data point). Cell-associated fluorescence increased 3-fold over the first 75 min of exposure and remained constant between 75 and 120 min despite repeated washes indicating that the secreted material removed by the acidified methanol wash (*D*, *extracellular*) was likely bound to proteins at the plasma membrane (*E*). *Scale bars*, 5 μm.

PAF). Surprisingly, PAF-AH α_1 protein levels decreased progressively over the first 30 min of PAF treatment and remained low until the end of the 90-min test period (Fig. 7*A*, *BN 52021*). Comparable results were observed in FR 49175-treated cultures (Fig. 7*A*, *FR 49175*). α_2 expression was not altered by BN 52021 or FR 49175 in that protein expression increased dramatically during the 15-min preincubation period in serum-free treatment media regardless of antagonist or vehicle administration and remained elevated over the 90 min PAF test period (Fig. 7*B*).

The finding that both compounds accelerate PAF degradation by reducing PAF-AH I α_1 subunit expression was unexpected. Two alternative, but not mutually exclusive, explanations lie in the possibility that this reduction in α_1 expression promotes formation of PAF-AH I α_2/α_2 homodimers and/or that PAF-AH II activity is increased. Following exposure to PAF in serum-free media, the catalytic composition of PAF-AH I would be expected to change from a predominance of α_1/α_1 homodimers in control cultures (Table I) to α_1/α_2 heterodimers and α_2/α_2 homodimers given the 8–10-fold increase in α_2 protein expression (Figs. 3 and 7). In cultures pretreated with BN 52021 or FR 49175, suppression of α_1 protein expression likely favors a more a rapid transition from α_1/α_1 to α_2/α_2 homodimers following PAF exposure. This hypothesis is supported by the dramatic increase in the α_2 to α_1 ratio observed 30–90 min after PAF exposure in BN 52021 and FR 49175-treated cultures relative to vehicle (Fig. 7*C*). Alternatively, in addition to effects on PAF-AH α_1, BN 52021 and/or FR 49175 may alter PAF-AH II activity, an enzyme with proven anti-apoptotic properties (26).

To address these possibilities, we performed three loss of function studies. First, we treated cells with 0.1 mM DFP to inhibit PAF-AH I α_1/α_1 and α_1/α_2 catalytic activity without changing the relative ratio of α_1 to α_2 protein expression (21, 23, 35). In the unlikely event that the anti-apoptotic effects of BN 52021 and FR 49175 are mediated by a loss of α_1 catalytic activity, then 0.1 mM DFP should be cytoprotective. Cells were exposed for 15 min (Fig. 4*C* and Fig. 8*A*) before addition of B-PAF. DFP did not affect B-PAF internalization (data not shown) but reduced B-PAF degradation by 38% 75 min after B-PAF exposure (Fig. 4*C*, *0.1 mM DFP, 75 min*). To ensure intracellular concentrations of DFP reached 0.1 mM by the time cells were exposed to PAF, we extended the preincubation

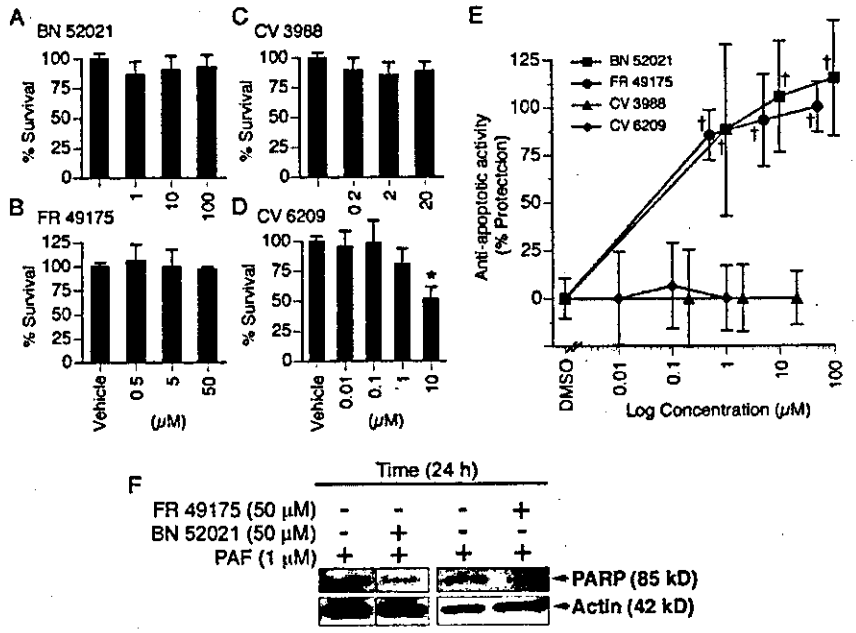

FIG. 5. **Anti-apoptotic actions of the PAF antagonists BN 52021 and FR 49175 but not CV-6209 or CV-3988 in PAFR-negative cells.** PC12-AC cells were pretreated for 15 min with 0.1% Me_2SO (*DMSO, vehicle*) or different concentrations of PAF antagonists and exposed to 0.1% EtOH (*A–D*) or PAF 1 μM (*E* and *F*) for 24 h. *A–E*, data are expressed as percent survival of vehicle-treated cultures. Results are reported as mean ± S.E. of n = 5–47 cultures per data point. BN 52021, FR 49175, and CV-3988 had no effect on the viability of vehicle-treated cultures. CV-6209 (10 μM) was toxic (*, $p < 0.05$). BN 52021 and FR 49175 but not CV-3988 or CV-6209 dose-dependently inhibited PAF-mediated death (†, $p < 0.05$; ††, $p < 0.01$). *F*, BN 52021 and FR 49175 inhibited PAF-mediated caspase 3 activation as assessed by PARP cleavage.

period from 15 to 30 min with no additional effects on the kinetics of PAF-AH inhibition (data not shown). Inhibition of PAF-AH I α_1/α_1 and α_1/α_2 catalytic activity did not alter survival of cells treated for 24 h with vehicle (Fig. 8*A*, *vehicle (0.1% EtOH)*) and did not intensify PAF-mediated cell death (Fig. 8*A*, *PAF*). These data suggest that PAF-AH I α_1 does not play a significant role in regulating PAF-induced apoptosis.

Second, to determine the role of PAF-AH II in control of PAF-mediated cell death, we treated cultures with PAF (1 μM) or PAF vehicle (0.1% EtOH) in the presence of DFP, the sulfhydryl blocking reagent (DTNB), or vehicle (PBS) (Figs. 4*C* and 8*A*). Cells were pre-exposed to 1 mM DFP or 1 mM DTNB for 15 (Figs. 4*C* and 8*A*) or 30 min (data not shown) before treatment with PAF or vehicle. Individually, DFP and DTNB were found to have no effect on the survival of vehicle-treated cells (Fig. 8*A*, *vehicle (0.1% EtOH)*). Increasing the DFP concentration from 0.1 to 1 mM inhibited 55% of B-PAF degradation within 75 min indicating that 17% of DFP-sensitive PAF-AH activity was PAF-AH II (Fig. 4*C*, *1 mM DFP, 75 min*). Despite this substantial inhibition of PAF hydrolysis (55%), PAF-mediated cell loss was intensified by only 8% (Fig. 8*A*, *1 mM DFP*). To confirm these results, we used a pharmacological agent that, unlike DFP, inhibits PAF-AH II but not PAF-AH I through different mechanisms. Exposure to 1 mM DTNB elicited the same results as 1 mM DFP (Fig. 8*A*, *DTNB*). To ensure complete inhibition of PAF-AH II, we exposed cells to both DFP and DTNB. Combination treatment reportedly abolishes activity of purified PAF-AH II (35). Preincubation in DFP and DTNB followed by 24 h of exposure to EtOH decreased vehicle-treated cell survival by 12% (Fig. 8*A*, *vehicle (0.1% EtOH)*). Combination of treatments reduced PAF-treated cell survival by 20%, likely the cumulative results of inhibitor toxicity (12%) and PAF-AH II inhibition (8%) (Fig. 8*A*, *PAF*). These findings suggest that (*a*) PAF-AH I α_1 activity is not anti-apoptotic and (*b*) that although PAF-AH II activity is cytoprotective, PAF-AH II plays a secondary role to PAF-AH I α_2 in regulating PAF-mediated apoptosis.

The data point to PAF-AH I α_2 as a potential therapeutic target to reduce apoptogenic PAF concentrations under diverse pathophysiological conditions. To confirm this role directly, we acutely suppressed α_2 expression using an RNAi strategy. PAF-AH I α_2-specific RNAi but not the scrambled control or transfection reagent alone reduced α_2 protein expression (Fig. 8*B*). Because we were unable to achieve >20% transfection efficiency, we could not knockdown PAF-AH I α_2 expression in all cells. To identify transfected cells, we co-transfected cultures with EGFP in combination with α_2-specific or scrambled siRNAs (Fig. 8*C*). To control for possible cytotoxic effects of siRNAs, parallel experiments were performed in which cultures were transfected with EGFP alone, and survival was expressed relative to EGFP-positive vehicle-treated cells. Most importantly, PAF-AH I α_2 RNAi down-regulation significantly enhanced PAF-mediated cytotoxicity (Fig. 8*C*).

DISCUSSION

PAF-like lipids have been implicated as key apoptotic second messengers induced by a variety of pathological stressors (6, 19, 20, 25, 26, 29, 30, 33, 40). Converging evidence points to PAFR activation of the conserved mitochondrial death pathway (6, 12, 18–20, 41). Our previous work has demonstrated that PAF can also transduce cell death independently of its G-protein-coupled receptor (11), but it is not known how cell death is regulated in the absence of PAFR. The importance of this apoptotic cascade is underlined by the fact that neurons express low levels to no PAFR (33, 42), and yet PAF is a principal mediator of neuronal loss in ischemia, encephalitis, epileptic seizure, meningitis, and human immunodeficiency virus-1 dementia (1–5). To provide mechanistic insight into this PAFR-independent pathway, we show the following. 1) PAF can initiate caspase-dependent cell death in the absence of it G-protein-coupled receptor. 2) The duration of PAF apoptogenic signaling is regulated by the α_2 subunit of PAF-AH I and, to a lesser extent, by PAF-AH II. 3) PAFR-independent cell death can be inhibited by two PAF antagonists: the gingkolide BN 52021 and the fungal derivative FR 49175 but not by CV-3988 or CV-6209. 4) Both BN 52021 and FR 49175 protect cells from PAF-induced cell death by reducing PAF-AH I α_1 protein levels indirectly promoting PAF-AH I α_2 homodimer activity.

Apoptotic PAF Signal Transduction in the Absence of PAFR—To provide mechanistic insight into how PAF transduces cell death in the absence of PAFR, we followed the internalization and metabolic fate of Bodipy fluorophore-conjugated PAF in PAF-sensitive cells (11, 43). PC12 cells express all of the components of both cytosolic PAF-AH enzymes (I and

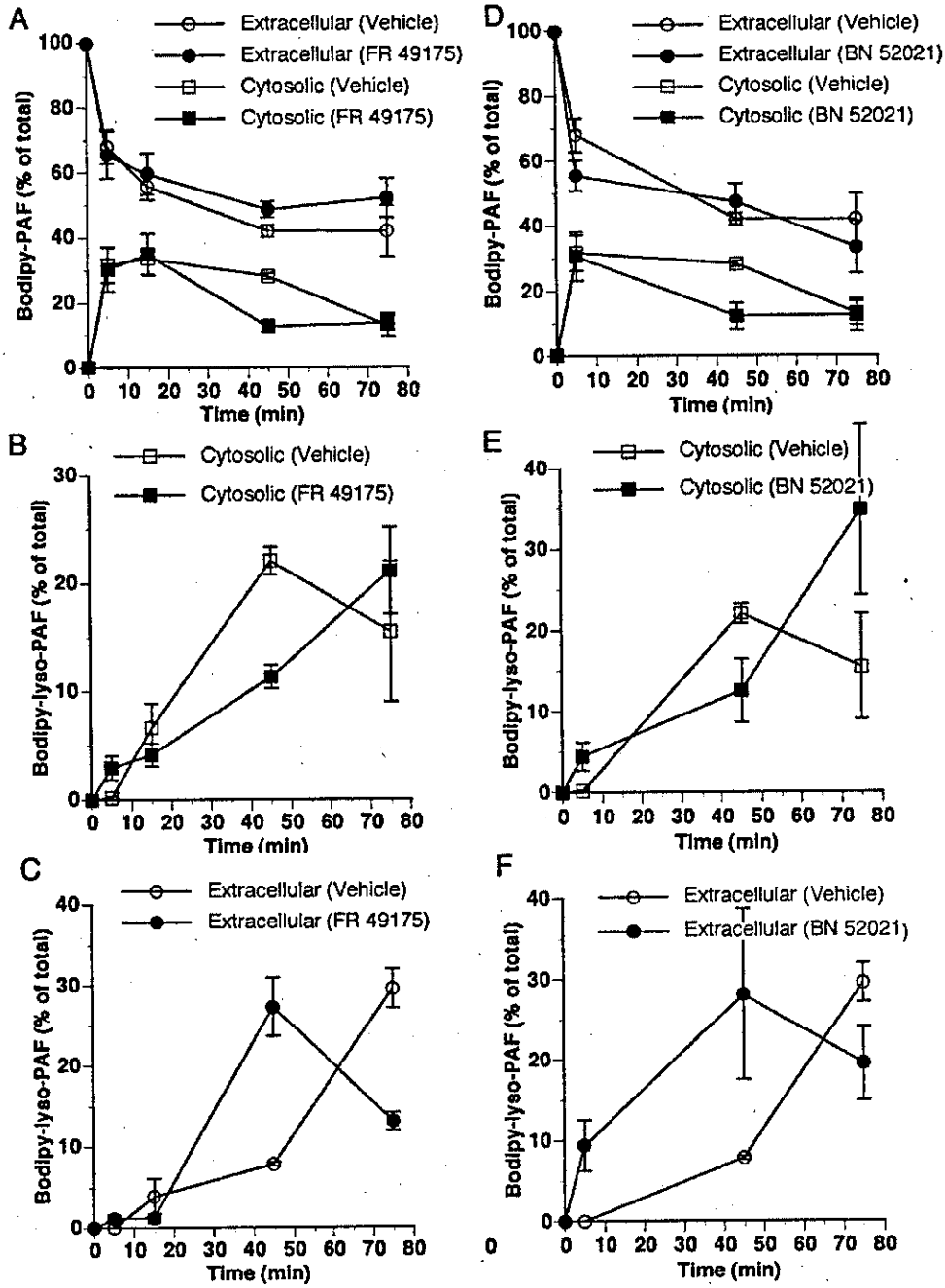

FIG. 6. **FR 49175 and BN 52021 accelerate the kinetics of PAF-AH activity.** PC12-AC cells were pretreated with FR 49175 (10 μM), BN 52021 (50 μM), or PBS (vehicle) for 15 min and then incubated with 1 μM B-PAF at 37 °C. Lipids were extracted from the extracellular and cytosolic fractions and separated by TLC. The relative fluorescence of B-PAF or B-*lyso*-PAF in each fraction is expressed as the percentage of the total fluorescent lipids recovered. Data represent the mean ± S.E. of $n = 4$ (FR 49175) or $n = 8$ (BN 52021) independent experiments conducted in replicate. *A*, FR 49175; *D*, BN 52021 had no effect on B-PAF internalization (*extracellular*), but cytosolic B-PAF levels were reduced within 45 min of exposure (*cytosolic*). *B* and *E*, the kinetics of B-PAF degradation and (*C* and *F*) release were accelerated in FR 49175- (*B* and *C*) and BN 52021 (*E* and *F*)-treated cells.

II) but not plasma PAF-AH or PAFR. Extracellular PAF was internalized by PC12 cells with a $t_{1/2}$ of ~5 min. Downstream activation of caspase 3 was initiated when cytosolic PAF concentrations were elevated by ~15–20 pM/cell. These findings complement previous work demonstrating that exposure to oxidative stressors triggers apoptogenic remodeling of membrane phospholipids into PAF-like lipids (26) and provide strong evidence that cytosolic accumulation of PAF and PAF-like lipids can trigger apoptotic death independently of PAFR. In fact, internalization of PAF mediated by PAFR endocytosis (36) may protect cells from this cell death cascade. Endocytosis of the PAF·PAFR complex triggers release of plasma PAF-AH from macrophages thereby reducing extracellular ligand concentrations (36).

Although we have yet to identify the effector proteins responsible for transducing increases in intracellular PAF concentration into downstream caspase activation, our data indicate that the temporal kinetics of PAF accumulation regulate the duration of apoptotic signaling and that PAFR-independent cell death is triggered by PAF and not by its immediate metabolite *lyso*-PAF. We found that intracellular PAF levels must remain elevated by approximately 60 min to elicit significant apoptotic death. Decreasing cytosolic concentrations to less than 10 pM/cell of exogenous PAF stops the cell death signaling. *lyso*-PAF,

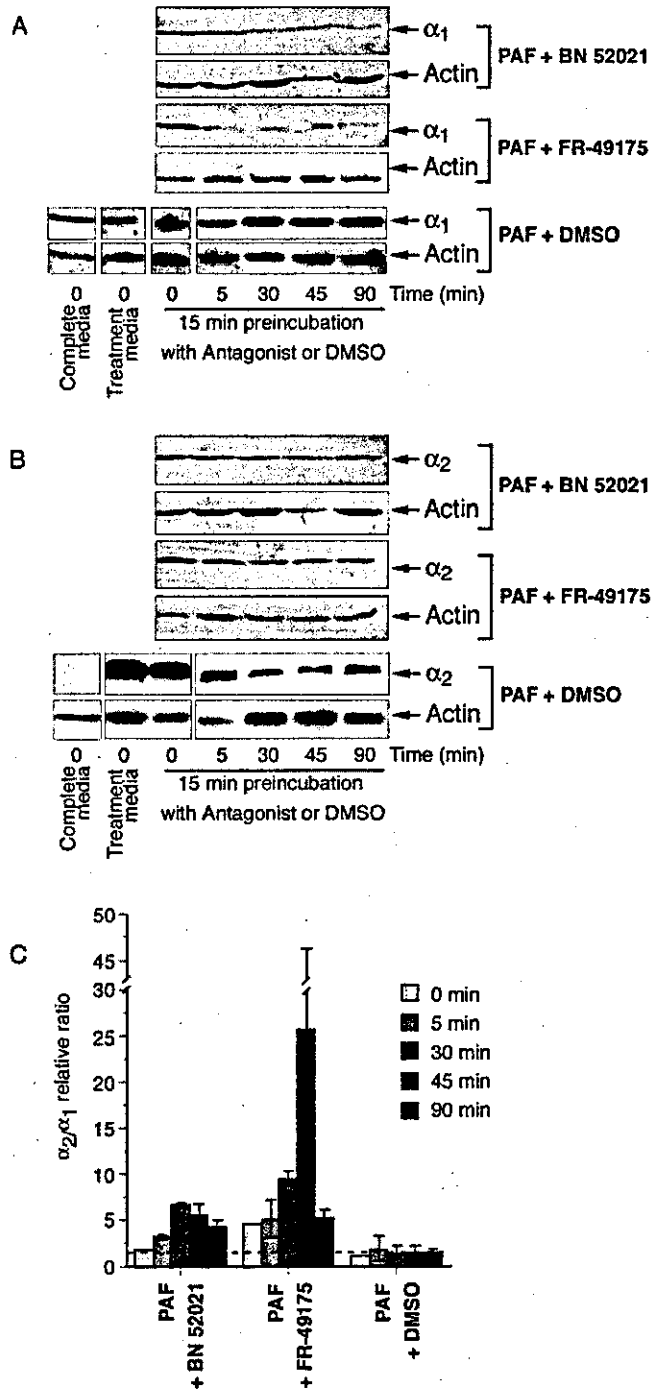

FIG. 7. **BN 52021 and FR 49175 increase the relative ratio of PAF-AH I α_2 to α_1 expression following PAF challenge.** PC12 cells were treated with PAF (1 μM) following a 15-min preincubation in the presence or absence of BN 52021 (50 μM), FR 49175 (50 μM), or vehicle (0.1% Me_2SO (*DMSO*)). Immunoblotting was performed for α_1 (*A*) or α_2 (*B*). BN 52021 and FR 49175 reduced α_1 expression (*A*) without affecting the α_2 induction (*B*). Blots were reprobed for actin as a loading controls (*A* and *B*). α_1 (*A*) and α_2 (*B*) protein levels were standardized to actin and expressed as a percent of the basal expression in cells cultured in complete media. *C*, the relative ratio of α_2 to α_1 protein following BN 52021 or FR 49175 revealed a stoichiometric increase in the levels of α_2 compared with α_1 relative to cells exposed to PAF in the absence of antagonist.

the immediate PAF metabolite, does not transduce downstream apoptotic induction given that equimolar concentrations of *lyso*-PAF are not cytotoxic and that the endogenous metabolite remains cell-associated without detectable effect. Accelerating the kinetics of PAF degradation with BN 52021 or FR 49175 reduces PAF concentration to sub-apoptotic levels (approximately >8 pM/cell) within 45 min and prevents PAF-induced caspase activation. The PAFR-specific antagonists CV-3988 and CV-6209 have no effect on PAF-mediated PAFR-independent cell death when administered at concentrations up to 20 times that of their reported IC_{50} antagonist activities (44–46). Most interestingly, the anti-cell death activities of the antagonists tested in this study (FR 49175 > BN 52021 > CV-3988 or CV-6209) are in direct opposition to their PAF antagonist potency in other biological assays (CV-6209 > CV-3988 > BN 52021 > FR 49175) (38, 44–47), suggesting that their PAFR-independent anti-apoptotic actions are inversely proportional to their affinity for PAFR.

We do not know how PAF is internalized by PC12 cells in the absence of its G-protein-coupled receptor. In addition to endocytosis as a PAF-PAFR complex, active trafficking of PAF across the plasma membrane is accomplished by a PAF-specific transglutaminase and by interaction with low affinity binding sites yet to be identified at the molecular level (14, 48). Passive PAF internalization is regulated by transbilayer movement (flipping) across the plasma membrane occurring as a result of physicochemical changes in membrane properties accompanying cellular activation (15). It has been suggested that PAF internalization in the absence of PAFR is not rapid enough to elicit acute biological activity in hematopoietic cells (36, 49). In this study, we present evidence that PAFR-independent PAF internalization by nonhematopoietic cells is indeed sufficient to trigger apoptotic cell loss.

PAF-AH α_2 Activity Is Anti-apoptotic—Administration of recombinant PAF-AH II or plasma PAF-AH and ectopic overexpression protects cells from death elicited by low density lipoprotein, glutamate, or oxidative stress (25, 26, 29–31). In this study, we show that PAF-AH I exerts similar cytoprotective effects with three important distinctions. First, the anti-apoptotic actions of PAF-AH I are subunit-specific. Under normal culture conditions, we found PAF hydrolysis in PC12 cells to be primarily mediated by the PAF-AH I α_1 subunit and to a lesser extent by PAF-AH II. Following serum deprivation and exposure to pathological PAF concentrations, PAF-AH I α_2 but not PAF-AH I α_1, protein expression is acutely up-regulated. By pharmacological inhibition using DFP and DTNB and by RNA interference, we found that PAF-AH I α_2 but not PAF-AH I α_1 activity reduces the duration of PAF-mediated apoptotic signaling. When cells were cultured under normal conditions, we found that cytosolic PAF-AH activity is PAF-AH 1 α_1/α_1 and α_1/α_2 (~70%) > PAF-AH I α_2/α_2 (~25%) > PAF-AH II (5%). When cells were deprived of serum and challenged with PAF, this activity profile shifted in favor of PAF-AH I α_2/α_2 (45%) > PAF-AH α_1/α_1 or α_1/α_2 (38%) > PAF-AH II (17%). Most surprisingly, pharmacological inhibition of α_1 enzymatic activity had no effect on PAF-mediated cell death, whereas suppression of α_2 induction by RNA interference significantly enhanced cell loss providing strong evidence for anti-apoptotic subunit specificity.

Second, PAF-AH I α_2 is mobilized as part of an endogenous cell survival response. These findings complement studies documenting the anti-apoptotic actions of plasma PAF-AH and PAF-AH II (8, 25, 26, 29–31). Moreover, we find that PAF-AH II is not able to compensate for a loss of PAF-AH I α_2 function. In fact, we were surprised to find that a 55% reduction in PAF hydrolysis observed 75 min after PAF challenge following DFP treatment only moderately enhanced PAF-mediated cell death. The kinetics of PAF-AH activation may explain the lack of significant PAF-AH II protection. PAF-AH α_2 is mobilized acutely in response to serum withdrawal, but an increase in DFP- or DTNB-sensitive PAF-AH II activity is only observed

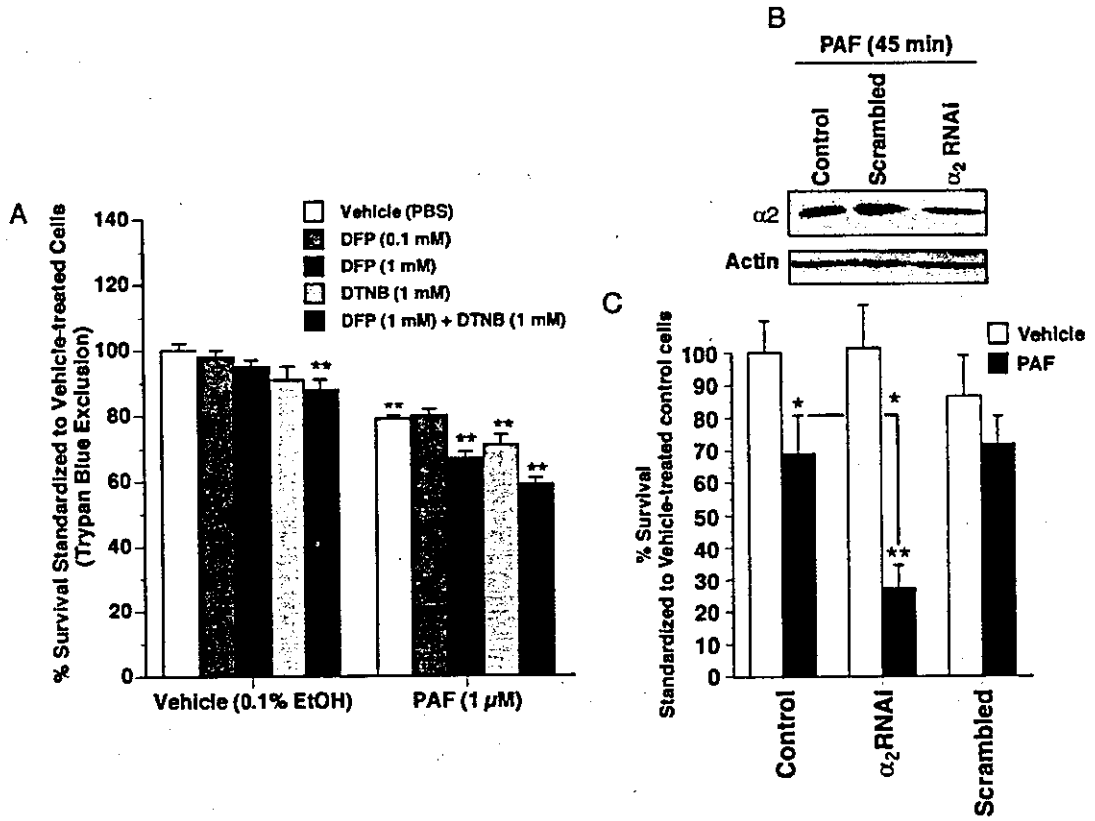

FIG. 8. **PAF-AH α_2 activity is anti-apoptotic.** *A*, PC12 cells were treated with PAF (1 μM) or ethanol (0.1%) at 37 °C for 24 h following 15 min of preincubation with DFP (0.1 mM), DFP (1 mM), DTNB (1 mM), or DFP (1 mM) + DTNB (1 mM) to abolish PAF-AH α_1 and PAF-AH II activity. Cell survival was assessed as described in Fig. 5. Inhibition of PAF-AH II but not PAF-AH α_1 activity moderately intensified PAF-mediated death. (ANOVA, *post hoc* Tukey tests, *, $p < 0.05$; **, $p < 0.01$). *B*, short interfering RNA oligonucleotides were employed to silence PAF-AH α_2. Western analysis for α_2 was performed at various time points after transfection following a 45-min treatment with PAF (1 μM) in serum-free treatment media. A partial knockdown in α_2 protein levels, consistent with the maximal 20% transfection efficiency, was detected 72 h after transfection (α_2 *RNAi*) compared with nontransfected cells (*control*) or cells that had been transfected with nonspecific scrambled RNAi (*scrambled*). β-Actin blot was performed as a loading control. *C*, PC12 cells were transfected with pEGFP-C1 (*control*) or co-transfected with pEGFP-C1 and α_2 RNAi (α_2 *RNAi*) or scrambled RNAi (*scrambled*). 72 h after transfection, cells were treated with PAF (1 μM) or vehicle (0.1% EtOH) for 24 h. Data are expressed as % survival of EGFP-positive cells standardized to vehicle-treated controls. Survival was reduced to 28% in cells transfected with α_2 RNAi compared to 70% in EGFP-transfected cells. *Asterisks* indicate statistically significant differences by Student's *t* test.

after 30–60 min of PAF exposure. Only PAF-AH I α_2 was found to reduce apoptogenic concentrations of cytosolic PAF within the first 30 min of exposure. PAF-AH II is mobilized as part of a delayed cell survival program possibly to ensure that "sub-apoptotic" PAF concentrations are maintained.

Third, and perhaps most importantly, the anti-apoptotic response afforded by shifting the PAF-AH I α_1 subunit expression in favor of α_2 can be enhanced by PAF antagonists. Pharmacological suppression of α_1 by BN 52021 or FR 49175 accelerates the kinetics of PAF deacetylation to *lyso*-PAF and protects cells from PAF-mediated apoptosis. Although it would at first appear counterintuitive that a reduction in PAF-AH subunit expression enhances PAF hydrolysis, these data are consistent with previous reports that BN 52021 inhibits PAF degradation under nonapoptotic culture conditions (48, 50). PAF-AH I α_2/α_2 is known to hydrolyze PAF more efficiently than α_1/α_1 homodimers, and it is likely that reducing PAF-AH α_1 coincident with PAF-AH α_2 induction would promote more rapid formation of α_2/α_2 homodimers, enhance PAF hydrolysis, and increase cell survival. Most interestingly, this phenomenon models the graded reduction in α_1 observed over the course of cerebral development by changing the predominant PAF-AH I catalytic composition from α_1/α_2 heterodimers in embryonic central nervous system to α_2/α_2 homodimers in adult brain (51). Our data suggest that this shift may render adult brain more resistant to PAF challenge than embryonic brain.

Summary—In summary, this study provides mechanistic evidence that sustained exposure to elevated intracellular PAF concentrations is sufficient to elicit apoptosis through a PAFR-independent cell death pathway. Previous studies have demonstrated that oxidative modification of membrane lipids during atherosclerotic injury, treatment with chemotherapeutic agents, ultraviolet B exposure, or excitoxicity is sufficient to produce PAF-like lipids (6, 19, 30, 31, 40). Our data suggest that these effects can occur in the absence of PAFR. To intervene in PAF-mediated death, we describe a novel anti-apoptotic function for PAF-AH I α_2 and II, and we identify two PAF antagonists that accelerate cytosolic PAF-AH I activity to inhibit PAF-mediated apoptosis.

Acknowledgments—We thank Tia Moffat for technical assistance and Jim Bennett for critical reading of this manuscript.

REFERENCES

1. Birkle, D. L., Kurian, P., Braquet, P., and Bazan, N. G. (1998) *J. Neurochem.* **51**, 1900–1905
2. Bazan, N. G. (1998) *Prog. Brain Res.* **118**, 281–291
3. Perry, S. W., Hamilton, J. A., Tjoelker, L. W., Dbaibo, G., Dzenko, K. A., Epstein, L. G., Hannun, Y., Whittaker, J. S., Dewhurst, S., and Gelbard, H. A. (1998) *J. Biol. Chem.* **273**, 17660–17664
4. Bate, C., Reid, S., and Williams, A. (2004) *J. Biol. Chem.* **279**, 36405–36411
5. Bate, C., Salmona, M., and Williams, A. (2004) *Neuroreport* **15**, 509–513
6. Li, T., Southall, M. D., Yi, Q., Pei, Y., Lewis, D., Al-Hassani, M., Spandau, D., and Travers, J. B. (2003) *J. Biol. Chem.* **278**, 16614–16621
7. Darst, M., Al-Hassani, M., Li, T., Yi, Q., Travers, J. M., Lewis, D. A., and Travers, J. B. (2004) *J. Immunol.* **172**, 6330–6335
8. Fukuda, Y., Kawashima, H., Saito, K., Inomata, N., Matsui, M., and Nakanishi, T. (2000) *Eur. J. Pharmacol.* **390**, 203–207

9. Grandel, K. E., Farr, R. S., Wanderer, A. A., Eisenstadt, T. C., and Wasserman, S. I. (1985) *N. Engl. J. Med.* **313,** 405–409
10. Ishii, S., and Shimizu, T. (2000) *Prog. Lipid Res.* **39,** 41–82
11. Brewer, C., Bonin, F., Bullock, B., Nault, M.-C., Morin, J., Imbeault, S., Shen, T. Y., Franks, D. J., and Bennett, S. A. L. (2002) *J. Neurochem.* **18,** 1502–1511
12. Southall, M. D., Isenberg, J. S., Nakshatri, H., Yi, Q., Pei, Y., Spandau, D. F., and Travers, J. B. (2001) *J. Biol. Chem.* **276,** 45548–45554
13. Tokuoka, S. M., Ishii, S., Kawamura, N., Satoh, M., Shimada, A., Sasaki, S., Hirotsune, S., Wynshaw-Boris, A., and Shimizu, T. (2003) *Eur. J. Neurosci.* **18,** 563–570
14. Bratton, D. L. (1993) *J. Biol. Chem.* **268,** 3364–3373
15. Bratton, D. L., Dreyer, E., Kailey, J. M., Fadok, V. A., Clay, K. L., and Henson, P. M. (1992) *J. Immunol.* **148,** 514–523
16. Sapir, T., Elbaum, M., and Reiner, O. (1997) *EMBO J.* **16,** 6977–6984
17. Marcheselli, V. L., Rossowska, M., Domingo, M. T., Braquet, P., and Bazan, N. G. (1990) *J. Biol. Chem.* **265,** 9140–9145
18. Hostettler, M. E., Knapp, P. E., and Carlson, S. L. (2002) *Glia* **38,** 228–239
19. Ma, X., and Bazan, H. E. P. (2001) *Curr. Eye Res.* **23,** 326–335
20. Tong, N., Sanchez, J. F., Maggirwar, S. B., Ramierez, S. H., Guo, H., Dewhurst, S., and Gelbard, H. A. (2001) *Eur. J. Neurosci.* **13,** 1913–1922
21. Manya, H., Aoki, J., Kato, H., Ishii, J., Hino, S., Arai, H., and Inoue, K. (1999) *J. Biol. Chem.* **274,** 31827–31832
22. Hattori, M., Adachi, H., Tsujimoto, M., Arai, H., and Inoue, K. (1994) *Nature* **370,** 216–218
23. Hattori, K., Adachi, H., Matsuzawa, A., Yamamoto, K., Tsujimoto, M., Aoki, J., Hattori, M., Arai, H., and Inoue, K. (1996) *J. Biol. Chem.* **271,** 33032–33038
24. Min, J.-H., Wilder, C., Aoki, J., Arai, H., Inoue, K., Paul, L., and Gelb, M. H. (2001) *Biochemistry* **40,** 4539–4549
25. Matsuzawa, A., Hattori, K., Aoki, J., Arai, H., and Inoue, K. (1997) *J. Biol. Chem.* **272,** 32315–32320
26. Marques, M., Pei, Y., Southall, M. D., Johnston, J. M., Arai, H., Aoki, J., Inoue, T., Seltmann, H., Zouboulis, C. C., and Travers, J. B. (2002) *J. Investig. Dermatol.* **119,** 913–919
27. Tjoelker, L. W., Eberhardt, C., Unger, J., Trong, H. L., Zimmerman, G. A., McIntyre, T. M., Stafforini, D. M., Prescott, S. M., and Gray, P. W. (1995) *J. Biol. Chem.* **270,** 25481–25487
28. Asano, K., Okamoto, S., Fukunaga, K., Shiomi, T., Mori, T., Iwata, M., Ikeda, Y., and Yamaguchi, K. (1999) *Biochem. Biophys. Res. Commun.* **261,** 511–514
29. Hirashima, Y., Ueno, H., Karasawa, K., Yokoyma, K., Setaka, M., and Takaku, A. (2000) *Brain Res.* **885,** 128–132
30. Ogden, F., DeCoster, M. A., and Bazan, N. G. (1998) *J. Neurosci. Res.* **15,** 677–684
31. Chen, C. H., Jiang, T., Yang, J. H., Jiang, W., Lu, J., Marathe, G. K., Pownall, H. J., Ballantyne, C. M., McIntyre, T. M., Henry, P. D., and Yang, C. Y. (2003) *Circulation* **107,** 2102–2108
32. Bligh, E. C., and Dyer, W. J. (1959) *Can. J. Biochem.* **37,** 911–917
33. Bennett, S. A. L., Chen, J., Pappas, B. A., Roberts, D. C. S., and Tenniswood, M. (1998) *Cell Death Differ.* **5,** 867–875
34. O'Flaherty, J., Redman, J., Schmitt, J., Ellis, J., Surles, J., Marx, M., Piantadosi, C., and Wykle, R. (1987) *Biochem. Biophys. Res. Commun.* **147,** 18–24
35. Hattori, K., Hattori, M., Adachi, H., Tsujimoto, M., Arai, H., and Inoue, K. (1995) *J. Biol. Chem.* **270,** 22308–22313
36. Ohshima, N., Ishii, S., Izumi, T., and Shimizu, T. (2002) *J. Biol. Chem.* **277,** 9722–9727
37. Pietri, S., Maurelli, E., Drieu, K., and Culcasi, M. (1997) *J. Mol. Cell. Cardiol.* **29,** 733–742
38. Yoshida, K., Okamoto, M., Shimazaki, N., and Hemmi, K. (1988) *Prog. Biochem. Pharmacol.* **22,** 66–80
39. Okamoto, M., Yoshida, K., Uchida, I., Kohsaka, M., and Aoki, H. (1986) *Chem. Pharm. Bull.* **34,** 345–348
40. Barber, L. A., Spandau, D. F., Rathman, S. C., Murphy, R. C., Johnson, C. A., Kelley, S. W., Hurwitz, S. A., and Travers, J. B. (1998) *J. Biol. Chem.* **273,** 18891–18897
41. Lu, J., Caplan, M. S., Saraf, A. P., Li, D., Adler, L., Liu, X., and Jilling, T. (2004) *Am. J. Physiol.* **286,** G340-G350
42. Mori, M., Aihara, M., Kume, K., Hamanoue, M., Kohsaka, S., and Shimizu, T. (1996) *J. Neurosci.* **16,** 3590–3600
43. Kornecki, E., and Ehrlich, Y. H. (1988) *Science* **240,** 1792–1794
44. Terashita, Z., Imura, Y., Takatani, M., Tsushima, S., and Nishikawa, K. (1987) *J. Pharmacol. Exp. Ther.* **242,** 263–268
45. Valone, F. H. (1985) *Biochem. Biophys. Res. Commun.* **126,** 502–508
46. Nunez, D., Chignard, M., Korth, R., Le Couedic, J. P., Norel, X., Spinnewyn, B., Braqueit, P., and Benveniste, J. (1986) *Eur. J. Pharmacol.* **123,** 197–205
47. Dupré, D. J., Le Gouill, C., Rola-Pleszczynski, M., and Stanková, J. (2001) *J. Pharmacol. Exp. Ther.* **2999,** 358–365
48. Lachachi, H., Plantavid, M., Simon, M. F., Chap, H., Braquet, P., and Douste-Blazy, L. (1985) *Biochem. Biophys. Res. Commun.* **132,** 460–466
49. Gerard, N. P., and Gerard, C. (1994) *J. Immunol.* **152,** 793–800
50. Lamant, V., Mauco, G., Braquet, P., Chap, H., and Douste-Blazy, L. (1987) *Biochem. Pharmacol.* **36,** 2749–2752
51. Manya, H., Aoki, J., Watanabe, M., Adachi, T., Asou, H., Inoue, Y., Arai, H., and Inoue, K. (1998) *J. Biol. Chem.* **273,** 18567–18572

THE JOURNAL OF BIOLOGICAL CHEMISTRY
Vol. 279, No. 30, Issue of July 23, pp. 30938–30944, 2004
Printed in U.S.A.

Scavenger Receptor Expressed by Endothelial Cells I (SREC-I) Mediates the Uptake of Acetylated Low Density Lipoproteins by Macrophages Stimulated with Lipopolysaccharide*

Received for publication, December 1, 2003, and in revised form, May 11, 2004
Published, JBC Papers in Press, May 15, 2004, DOI 10.1074/jbc.M313088200

Yoshiaki Tamura‡, Jun-ichi Osuga‡, Hideki Adachi§, Ryu-ichi Tozawa‡, Yasukazu Takanezawa¶, Ken Ohashi‡, Naoya Yahagi‡, Motohiro Sekiya‡, Hiroaki Okazaki‡, Sachiko Tomita‡, Yoko Iizuka‡, Hiroyuki Koizumi¶, Toshihiro Inaba‖, Hiroaki Yagyu‖, Nobuo Kamada, Hiroshi Suzuki‡‡, Hitoshi Shimano§§, Takashi Kadowaki‡, Masafumi Tsujimoto§, Hiroyuki Arai¶, Nobuhiro Yamada§§, and Shun Ishibashi‡‖¶¶**

*From the ‡Department of Metabolic Diseases, Faculty of Medicine, University of Tokyo 7-3-1 Hongo, Bunkyo-ku, Tokyo 113-8655, Japan, the §Laboratory of Cellular Biochemistry, Institute of Physical and Chemical Research (RIKEN), Wako-shi, Saitama 351-0198, Japan, the ¶Department of Health Chemistry, Graduate School of Pharmaceutical Science, University of Tokyo 7-3-1 Hongo, Bunkyo-ku, Tokyo 113-0033, Japan, the ‖Department of Internal Medicine, Jichi Medical School, 3311-1 Yakushiji, Minamikawachi-machi, Kawachi-gun, Tochigi 329-0498, Japan, the **Chugai Research Institute for Medical Science Incorporated, 1-135 Komakado, Gotenba, Shizuoka 412-8513, Japan, the ‡‡Unit for Functional Genomics, National Research Center for Protozoan Diseases, Obihiro University of Agriculture and Veterinary Medicine, Nishi-2, Inada, Obihiro, Hokkaido 080-8555, Japan, and §§Metabolism, Endocrinology, and Atherosclerosis, Institute of Clinical Medicine, University of Tsukuba, 1-1-1 Tennodai, Tsukuba, Ibaraki 305-8575, Japan*

Scavenger receptor expressed by endothelial cells I (SREC-I) is a novel endocytic receptor for acetylated low density lipoprotein (LDL). Here we show that SREC-I is expressed in a wide variety of tissues, including macrophages and aortas. Lipopolysaccharide (LPS) robustly stimulated the expression of SREC-I in macrophages. In an initial attempt to clarify the role of SREC-I in the uptake of modified lipoproteins as well as in the development of atherosclerosis, we generated mice with a targeted disruption of the *SREC-I* gene by homologous recombination in embryonic stem cells. To exclude the overwhelming effect of the type A scavenger receptor (SR-A) on the uptake of Ac-LDL, we further generated mice lacking both SR-A and SREC-I (*SR-A*$^{-/-}$;*SREC-I*$^{-/-}$) by cross-breeding and compared the uptake and degradation of Ac-LDL in the isolated macrophages. The contribution of SR-A and SREC-I to the overall degradation of Ac-LDL was 85 and 5%, respectively, in a non-stimulated condition. LPS increased the uptake and degradation of Ac-LDL by 1.8-fold. In this condition, the contribution of SR-A and SREC-I to the overall degradation of Ac-LDL was 90 and 6%, respectively. LPS increased the absolute contribution of SR-A and SREC-I by 1.9- and 2.3-fold, respectively. On the other hand, LPS decreased the absolute contribution of other pathways by 31%. Consistently, LPS did not increase the expression of other members of the scavenger receptor family such as CD36. In conclusion, SREC-I serves as a major endocytic receptor for Ac-LDL in LPS-stimulated macrophages lacking SR-A, suggesting that it has a key role in the development of atherosclerosis in concert with SR-A.

Scavenger receptors mediate the endocytosis of chemically modified lipoproteins such as acetylated low density lipoprotein (LDL),[1] thereby contributing to the development of atherosclerosis (1). The scavenger receptor gene family comprises a series of unlinked genes encoding membrane proteins with diverse ligand binding activity (2). The class A type I/type II scavenger receptor (SR-A) is the prototype receptor belonging to this family (3) and accounts for ~80% of the uptake of Ac-LDL in macrophages (4, 5).

Recently, we identified scavenger receptor expressed by endothelial cells I (SREC-I), which encodes a protein of 830 amino acids and binds fluorescent DiI-labeled Ac-LDL when expressed in Chinese hamster ovary cells (6), and its paralogous gene, *SREC-II* (7). The SREC-I protein is composed of an N-terminal extracellular ligand binding domain with seven epidermal growth factor receptor-like cysteine pattern signatures, a membrane-spanning domain, and an unusually long C-terminal cytoplasmic domain that includes a Ser/Pro-rich region followed by a Gly-rich region. SREC-II encodes an 834-amino acid protein with 35% homology to SREC-I. Although SREC-II has little activity to internalize modified LDL, SREC-I-expressing fibroblasts are intensely aggregated with SREC-II-expressing fibroblasts, indicating the association of SREC-I and SREC-II (7). However, the precise functions of these two proteins are currently unknown.

In atherosclerotic lesions, macrophages are laden with lipids and immunologically activated (8). In line with this, the development of atherosclerosis is accelerated by LPS (9), a major component of Gram-negative bacteria that stimulates the production of various cytokines *in vivo*, thereby contributing to the pathogenesis of endotoxin shock (10). Conversely, the absence of toll-like receptor 4, a receptor for LPS, inhibits its progression (11). These considerations have prompted us to examine the effects of LPS on the expression of SREC-I. In the present study, we show that LPS robustly stimulated the expression of

* This work was supported by a grant-in-aid for Scientific Research from the Ministry of Education, Science, and Culture and by the Takeda Medical Research Foundation. The costs of publication of this article were defrayed in part by the payment of page charges. This article must therefore be hereby marked "*advertisement*" in accordance with 18 U.S.C. Section 1734 solely to indicate this fact.

¶¶ To whom correspondence should be addressed: Division of Endocrinology and Metabolism, Department of Internal Medicine, Jichi Medical School, 3311-1 Yakushiji, Minamikawachi-machi, Kawachi-gun, Tochigi 329-0498, Japan. Tel.: 81-285-58-7355; Fax: 81-285-40-6035; E-mail: ishibash@jichi.ac.jp.

[1] The abbreviations used are: LDL, low density lipoprotein; SR-A, class A type I/type II scavenger receptor; SR-BI, class B type I scavenger receptor; SREC, scavenger receptor expressed by endothelial cells.